Dear Dr. Haywood,

We'd like to thank you for reviewing our paper. We have carefully considered your comments and suggestions, and revised the manuscript accordingly. Thanks to your comments/suggestions, we felt that the manuscript is significantly improved. Point-to-point replies to your review are listed below.

- *Section 2.1. In thick biomass burning regions, there is some evidence that the AOD derived from the CALIOP 532nm channel may be attenuated to an extent where it does not penetrate down to the bottom of the aerosol layer leading to too small AODs being retrieved (AGU meeting, Jethva pers. Comm..). This may lead to a low bias in the AOD derived from CALIOP which may bias the results presented in this paper.... However, this work has not yet to my knowledge been published. I leave it to the authors whether they want to follow up on this and include a caveat.*

Reply:

The other two reviewers have also raised similar questions. Indeed, some recent studies, for example [*Jethva et al*., 2014], suggest that the current CALIOP operational smoke AOD retrieval (V3.01) is probably biased low relative to results based on other methods. In addition to the issue you mention, solar background noise may also contribute to this bias [*Meyer et al*., 2013]. The emerging retrievals from passive sensors [e.g., *Waquet et al*., 2009; *Torres et al*., 2012; *Jethva et al*., 2013] will definitely help resolve this issue. In the revised manuscript, a brief discussion is added to Section 2.1 to note this issue and explain the cause. We agree with you and the other reviewers that it is important to estimate the impact of CALIOP retrieval bias on the ACA DRE computation. In the revised manuscript, we add a new section (section 3.4) specifically on the relevant uncertainty analysis.

From a technical perspective, the uncertainty analysis is simple, as long as the nature and magnitude of uncertainties in the input data are known. For example, the aforementioned CALIOP AOD bias can be accounted for in uncertainty analysis by shifting the original PDF of AOD, $p(\tau_a)$ to a perturbed PDF $\tilde{p}(\tau_a)$. Then the impact of the AOD bias can be estimated through comparison of results between the original and perturbed PDF (i.e., $\langle DRE \rangle_{ACA}$ vs. $\langle \widetilde{DRE} \rangle_{ACA}$). Note that $\langle DRE \rangle_{ACA}$ and $\langle \widetilde{DRE} \rangle_{ACA}$ can be obtained with a single computation because they are both derived by integrating over $DRE(\tau_c, \tau_a)$, only using different weights. In this regard, our method is much more efficient than the pixel-by-pixel method, in which uncertainty is estimated by perturbing individual pixels. What is more challenging is to estimate to what extent the CALIOP retrieval underestimates the ACA AOD. This is actually a question beyond the scope of this study. A previous study by [*Meyer et al*., 2013] found that daytime CALIOP AOD retrievals are systematically smaller than nighttime retrievals, probably because of the daytime solar background issue. In the light of this finding, Meyer et al. (2013) shifted the CALIOP AOD retrievals by a factor of 1.5 to estimate the impact of this AOD bias on the DRE of

ACA. A more recent case study by [*Jethva et al*., 2014] suggest that CALIOP AOD is biased low by a factor of 4 to 6.

In the revised manuscript, we estimated the impact of CALIOP AOD retrieval uncertainty on DRE based on [*Meyer et al*., 2013; *Jethva et al*., 2014]. Following [*Meyer et al*., 2013], we multiplied the CALIOP retrieved above-cloud AOD by 1.5 and computed the DRE based on the 1.5x AOD. In the other test, we multiplied the CALIOP retrieved above-cloud AOD by a factor of 5 as suggested in [*Jethva et al*., 2014]. The regional and seasonal mean DRE of ACA increased from the original value of 6.39 W m^{-2} to 9.57 W m^{-2} in the x1.5 test and to 30.87 W m^{-2} in the x5.0 test. We must note that this is a very rough estimate. Nevertheless, the DRE based on 50% enhancement of CALIOP AOD seems to agree reasonably with the value, 9.2±6.6 W m^{-2} , reported in [*Wilcox*, 2012]. Interestingly, the scaling of AOD has little impact on RFE in both cases (53.09 W m^{-2} AOD^{-1} in the x1.5 case and 51.24 W m^{-2} AOD^{-1} in the x5.0 case), which apparently suggests a near linear relationship between DRE and AOD as also noted in [*Meyer et al.*, 2013] and[*Wilcox*, 2012].

- *P10000, l5. Section 3.1., and section 3.2, l17. Having had a look at the Omar et al (2009) paper, and the Meyer et al (2013) paper, I'm a little confused about the aerosol model. It appears that you are interested in the two most absorbing aerosol types, (1) smoke and (2) polluted dust, as evidenced by the imaginary part of the refractive index in Omar et al (2009), Table 1. You state that the Mie scattering calculations are based on "the aerosol model in Meyer et al (2013)". The Meyer model appears to be based on the assumption that the overlying aerosol is the CALIOP determined smoke aerosol (based on the imaginary part of the refractive index that is assumed). Is there a different model used for polluted dust or do you just use a single assumed model for the polluted dust and the smoke aerosols classified by CALIOP? I would suggest that aerosol off the coast of the Sahel/Sahara where dust is mixed with BB during DJF (see e.g. schematic diagram and results from the AMMA/DABEX field campaign, Haywood et al., JGR, doi:10.1029/2008JD010077, 2009, Fig 12) that the column BBA/dust single scattering albedo may be greater than 0.9 as the dust is essentially non-absorbing (Omar's paper suggests this).*

Reply:

Yes, we *"just use a single assumed model for the polluted dust and the smoke aerosols classified by CALIOP"* in our computations. This is a choice made to keep our result consistent with and comparable to [*Meyer et al*., 2013]. The model in [*Meyer et al*., 2013] is a smoke aerosol model based on the MODIS Collection 5 Aerosol Product (MOD04) [*Levy et al*., 2009]. It may not be suitable for other types of ACAs. However, as we mentioned in the paper, our method can be easily extended to other aerosol models. In fact, we have recently implemented the six operational CALIOP aerosol models described in [*Omar et al*., 2004] in our method. Some preliminary results are shown in Figure 1, which shows the bulk scattering properties of the dust, smoke and polluted dust aerosol models in [*Omar et al*., 2004] and the corresponding ACA DRE computed using our new method applied on 4 years of CALIOP and MODIS data. Although the results

are too preliminary for any definitive conclusions, they clearly demonstrate that our method is flexible and can used for other aerosol types. In future studies, we will investigate the DRE of various aerosol types over the "hot spots" of ACA over the globe. The *Sahel/Sahara* region, where Sahel dust from north mixes with smoke from the south is certainly an interesting region to look at.

On the other hand, Figure 1 also indicates that any uncertainty in the aerosol microphysical and optical model can result in substantial errors and uncertainties in DRE computation. The aerosol models in [*Omar et al*., 2004] are based on AERONET data, which are limited to clear-sky observations. It remains unclear to what extent those models can represent above-cloud aerosols. There is undoubtedly a need for in situ and remotely sensed measurements from field campaigns to improve our understanding of the microphysical and optical properties of ACA, which will in turn help us understand their DRE.

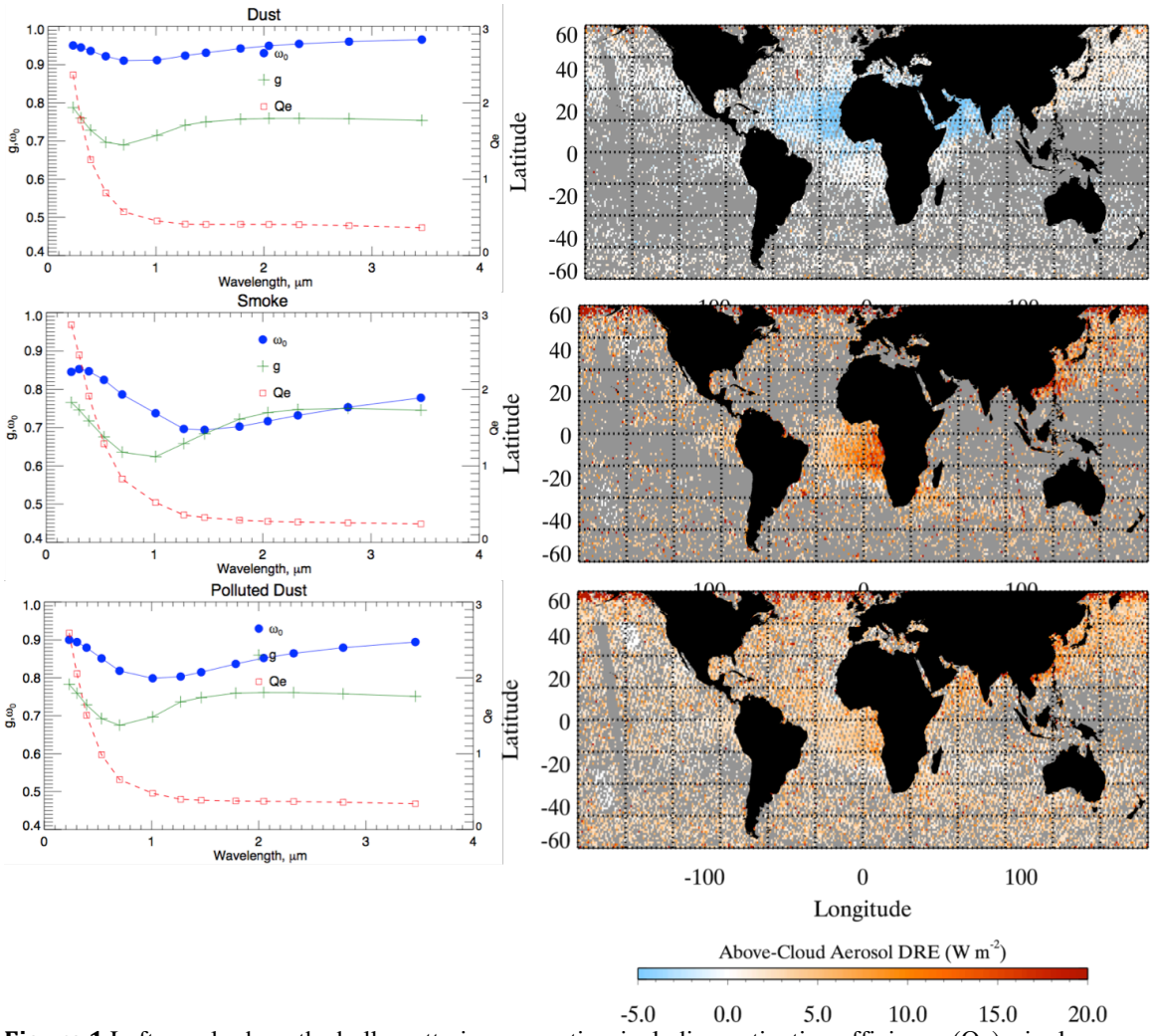

Figure 1 Left panels show the bulk scattering properties, including extinction efficiency (Qe), single-scattering albedo (ω) and asymmetry factors (g) of the dust, smoke and polluted dust aerosols computed using Mie code based on the microphysical models described in **[*Omar et al.*, 2009]**. Right panels show the corresponding ACA DRE computed using our new method from four years of CALIOP and MODIS data.

- *P 10004, l22-26. I would be tempted to swap the results round: you've gone to the trouble of correcting for the underlying COD underestimate, so why not show these?*

- *Fig 3. You show comparisons against the pixel-pixel approach. Why not show a scatter plot i.e. a vs c and b vs d. Then you could do a short statistical analysis to see if the relationship is indeed linear.*

Reply:

Following your suggestions, in the revised version we showed the results based on the corrected-COD in Figure 3 and 4. In addition, we added scatter plots along with simple linear fit results in the new Figure 3 e and f which confirm that the relationship is indeed linear with very high correlation coefficient.

- *Section 4, p10004, l 28. I like that you've gone to RFE. I don't know whether you have enough statistics to go slightly further – to RFE/COD in Wm-2/ACA AOD/COD. This would mean that you can actually start to make comparisons against models which underestimate the stratus cloud deck AOD for whatever reason. It could be a useful num ber to have.....*

Reply:
Very interesting idea. Following your suggestion, we compute the RFE/COD over the SE Atlantic region. Shown in Figure 2c below is the multi-year seasonal mean RFE/COD. As you can see, in contrast to DRE and RFE which are mostly positive values (see Figure 3 of the paper), RFE/COD over this region has both positive and negative values. A closer look of the above-cloud AOD (Figure 2 a) and below-aerosol COD (Figure 2 b) indicates that those negative RFE/COD values are mostly associated with thinner clouds. This is probably because those negative RFE values are amplified by the small COD value in the denominator in the RFE/COD averaging, which in turn leads to the negative RFE/COD. This is an interesting result, but we are not sure it is helpful for this study. So we just leave this result in this reply.

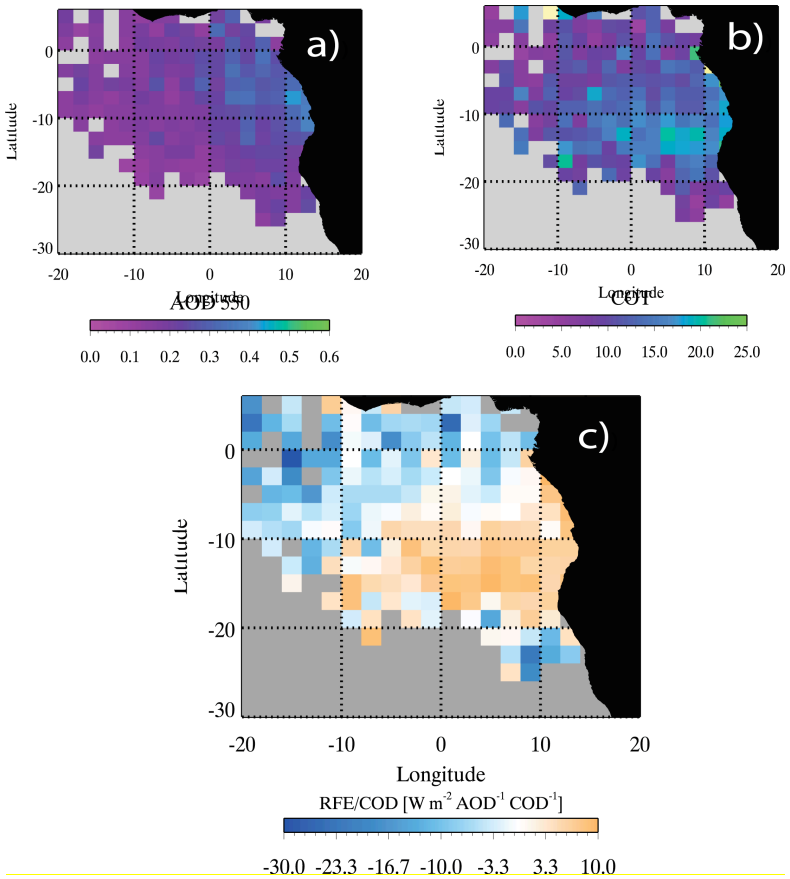

Figure 2 a) above-cloud AOD (@550nm) derived from CALIOP data, b) below cloud COD from MODIS and c) RFE/COD

- *#1. I'm not sure whether the SSA of ~0.9 is used for both smoke and polluted dust*

(see comments above). The negative DREs that you refer to at the top of p10007 are presumably because the underlying cloud is so thin that it doesn't impact the effective surface reflectance enough to tip over the balance point from negative to positive forcing. You may want to clarify this point with a few more words.

Reply: About the aerosol model, please see our reply above. We have added some brief discussion on the negative DRE.

- *#2. I think that something should be said about how best to make use of the data that is presented in the paper. You should highlight that the measurements that you make are valid for a certain time of the day (A-train overpass). The diurnal cycle of cloud in the SE Atlantic is quite high, with less cloud at the time of the AQUA overpass than e.g. earlier on in the day (stratocumulus burn off) so models should endeavour to compare against a similar time period.*

Reply:

Thanks for the suggestion. In the revised manuscript, we reminded the readers again at the end of Section 4 that: the results in this study are seasonal mean *instantaneous* DRE at A-Train crossing time (1:30PM local time) based on CALIOP above-cloud AOD and corrected Aqua MODIS below-aerosol COD retrievals. The aerosol model described in [*Meyer et al.*, 2013] is used in this study. All these factors should be considered when comparing the results in this study with those in other studies [e.g., *Chand et al.*, 2009; *de Graaf et al.*, 2012; *Wilcox*, 2012].

In addition, we added the following discussions:

In this study, we focus on the computation of instantaneous DRE. To obtain diurnally averaged DRE, technically speaking one would simply need to integrate over time the instantaneous DRE. However, it is important to note that, in addition to diurnal variation of solar zenith angle, aerosol and cloud properties may also have significant diurnal cycles. In fact, as you pointed out, the cloud fraction of stratocumulus regimes, such as the South East Atlantic region, has a strong diurnal cycle (15~35% of diurnal mean value) driven by cloud solar absorption [*Wood et al.*, 2002]. A recent study by [*Min and Zhang*, n.d.] indicates that using a constant cloud fraction based on Aqua-MODIS observation tends to result in significantly underestimated diurnal mean DRE even if the diurnal variation of solar zenith angle is considered in the computation. Therefore, the diurnal variation of cloud properties is an important factor to consider in the inter-comparison of DRE computations based on different datasets and inter-comparison between observational study and modeling results.

- *#3. I think that you are missing an important reference – that of de Graaf et al. (2011) who use SCIAMACHY to show the spectral distribution of the DRE derived above clouds. It would be even more interesting to see what you're modelled spectral dependence of the DRE over cloud is and whether your spectral*

dependence derived from an assumed model looks like what is derived from SCIMACHY (that doesn't assume an aerosol model). My suspicion is that the constant refractive index assumption that is used in the model (particularly the imaginary part), may lead to not enough absorption in the UV (absorption of brown organic carbon likely has a role in this), and hence the DREs and RFEs may be rather smaller than if a wavelength dependent refractive index

Reply:

Thanks for the reference. We cited *de Graaf et al. (2011)* in the revised manuscript. The main purpose of this study is to demonstrate the methodology. We will compare DRE of ACA based on our method with other studies, such as *de Graaf et al. (2011)*, in future research.

Typos/minor comments:

- *P9996, l21. I would remove most recently as you've already discussed this paper in the preceding paragraph.*

Reply: we combined this paragraph with the previous one as they are both talking about Meyer et al. 2013 paper.

- *P9998, l7. assumption -> assumptions*

Reply: Changed.

- *P10001, l3. While Constantino and Breon find no correlation between above-cloud AOD and below-aerosol COD, I think it worth stating that they do find a relationship between cloud fraction and aerosol index. Otherwise the reader may infer that there is no correlation and/impact at all.*

Reply: We clarified this point in section 3.1.

- *P10003, l5. (e.g. .....) should be just after the first bracket.*

Reply: this seems to be a bug of the citation management software I use. I've changed the citation.

Dear Dr. Jethva,

We'd like to thank you for reviewing our paper. We have carefully considered your comments and suggestions, and revised the manuscript accordingly. Thanks to your comments/suggestions, we felt that the manuscript is significantly improved. Point-to-point replies to your review are listed below.

- *While the method itself appears to be promising and more efficient than the conventional PBP approach, it requires a combination of the existing aerosol and cloud products available operationally from the A-train sensors. So naturally, the accuracy of the DRE estimation directly depends on the level of uncertainty associated with each product. For instance, the above-cloud aerosol optical depth retrieved by the CALIOP aerosol algorithm is significantly biased low in comparison to other passive sensors/techniques [Jethva et al., 2014, GRL, accepted]. This will lead to a low bias in the correction/adjustment applied to the MODIS cloud optical depth and ultimately to the estimation of DRE. While the results of this method strongly depend on the accuracy of the ingested retrieval products, I assert here that the methodology itself stands alone and is unaffected.*

Reply:

Indeed, as we state, our method "*requires a combination of the existing aerosol and cloud products available operationally from the A-train sensors. So naturally, the accuracy of the DRE estimation directly depends on the level of uncertainty associated with each product.*" There is no difference between our new method and other methods, for example pixel-by-pixel computation, in this regard.

As your recent paper *[Jethva et al., 2014, GRL, accepted]* shows, there are still substantial uncertainties in the current above-cloud aerosol properties retrievals. Uncertainty in the input data (e.g., CALIOP AOD) will certainly lead to uncertainty in the ACA DRE estimate. We need to demonstrate that our method is able to provide an estimate of uncertainty in DRE based on reasonable estimate of uncertainty sources. In the revised manuscript, we add a new Section 3.4 on uncertainty analysis. Please refer to our response on a related question by reviewer Haywood.

- *One of the few things I couldn't understand completely is how the CALIOP lidar measurements which have very limited samplings in 1 deg box have been extended to all MODIS 1 km cloud retrieval. Do authors simply average the CALIOP above-cloud AOD and applies to the entire 1 deg region? If so, the spatial variation in AOD outside the lidar's line of measurements can introduce uncertainty in the estimation of DRE. The assumptions of the spectral aerosol properties, the most important one is the single- scattering albedo can be an additional source of uncertainties. But again, I see that the main point of the paper is to demonstrate the method using existing retrieval products. When*

comparing with the PBP approach of Meyer et al. (2013), do author include all the MODIS measurements intercepted in 1 deg region or just the retrieval along the CALIOP overpass?

Reply:

We do **not** "*simply average the CALIOP above-cloud AOD and applies to the entire 1 deg region"*. We actually use CALIOP product to obtain the PDF of above-cloud AOD, $p(\tau_a)$ along CALIOP track within a grid-box and use it in the DRE and RFE computations based on Eq. (2). However, we **do** assume that the along-track AOD PDF represents the statistics of the whole grid-box including the off-track part. As you also noted, this is not a limitation of our method, but an inherent limitation of CALIOP data.

As we mentioned in the Summary and Discussion section, several novel methods have been developed to retrieve above-cloud aerosol properties from passive sensors [*Waquet et al*., 2009; *Torres et al*., 2012; *Jethva et al*., 2013]. These methods will be able to provide the AOD statistics over the entire grid-box, which can be used in our method. In fact, the advantage of our method over the pixel-by-pixel method, will be more prominent in such cases. For example, if the color-ratio method [*Jethva et al*., 2013] were applied to the SEVIRI observations, one could potentially obtain above-cloud AOD retrievals over the SE-Atlantic region (a 40x50 degree box) every 15 minutes at the spatial resolution of several km. Assuming the region is 50% cloudy, the sampling rate can be easily over 10 million pixels per day. The computation cost would be very high if DRE computations were to be performed on-line on a pixel-by-pixel basis, especially for multi-year climatology studies. In such situations, our method provides an efficient alternative. We actually hope that the above-cloud aerosol properties retrievals from passive sensors [*Waquet et al*., 2009; *Torres et al*., 2012; *Jethva et al*., 2013] can become operational and available to the public in the near future, and look forward to working with these teams to use their data for better understanding of ACA DRE.

Specific comments:

- *Page 9995, line 25: author can also add Meyer et al. (2013)*

- *Page 9996, line 16: add Wilcox et al. (2009) and Jethva et al. (2013)*

Reply: References added

- *Page 9997, line 5: I think Meyer et al. (2013) also used pre-computed look-up-table for estimating the ACA DRE. Please confirm.*

Reply: No, in Meyer et al. (2013) DRE computation is done using RRTMG model pixel by pixel.

- *Page 9999, line 21: I assume here that the size of grid box is 1 deg. Please confirm.*

Reply: The size of grid-box can be arbitrary

- *Page 10000, line 17: If I understand the present method correctly, the above-cloud AOD and layer (top/bottom) information retrieved from CALIOP in a 1 deg grid box is assumed to be uniform and therefore applied to the entire 1 deg grid observations of COD/CTP from MODIS. If above is true, then it will have implications on estimated DRE for ACA situations. In comparison, CALIOP observations are significantly under-sampled than those of MODIS Level-2 1-km retrievals. Applying the mean values of CALIOP retrievals to the entire grid box may mask the natural spatial variability in aerosol properties.*

Reply*:* As we have already clarified earlier, we do **not** "*simply average the CALIOP above-cloud AOD and applies to the entire 1 deg region"*. We actually use the CALIOP product to obtain the PDF of above-cloud AOD, $p(\tau_a)$ along CALIOP track within a grid-box and use it in the DRE and RFE computations based on Eq. (2). However, we **do** assume that the along-track AOD PDF represents the statistics of the whole grid-box including the off-track part. As you also noted, this is not a limitation of our method, but inherent limitation of CALIOP data.

- *Page 10001, line 1-5: I read the abstract of Costantino and Breon. They found strong effects of absorbing aerosols on cloud fraction when aerosols are located above cloud top. This is perfectly in line with the conclusion of Wilcox et al. (2010,2012) papers: a heated layer increases the stability and thus reduces the entrainment from top, thus preserving or even increase LWP and COD. But, now my argument goes like this: if above hypothesis is at work in reality, the apparent COD retrieved by MODIS inherently carries this information (increased LWP/COD) which is further corrected for the above- cloud aerosol presence using CALIOP observations. So, I believe at the end of the day it is reasonable to assume that the above-cloud AOD and underlying COD are statistically independent.*

Reply: Thank you for you comments. Please see our response to reviewer Wilcox on a related question

- *Page 10002, line 7: spectral aerosol properties?*

Reply: changed to "broadband aerosol scattering "

- *Page 10003, line 1-3: "..DRE of ACA is largely insensitive to cloud effective radius..."*

Reply: changed as suggested.

- *Page 10003, section 3.3, 1st paragraph: The accuracy of the COD correction obviously relies on the accuracy of the above-cloud AOD and assumed model. Recently, in an inter-comparative analysis of the above-cloud AOD retrieved from four sensors on board A-train satellites [Jethva et al., 2014, GRL, accepted], we find that the CALIOP 532-nm ACAOD is consistently under-estimated by a factor of 5 or more relative to the retrievals from passive sensors (MODIS, OMI, POLDER). Such a large bias in AOD will lead to erroneous COD corrections and ultimately biased estimation of DRE. However, I see here that the main point of this paper is to demonstrate the method for the DRE estimation and therefore inaccuracy in the CALIOP/MODIS retrievals used in this work should not be treated as the weakness of the original method. I suggest author to add a small section or at least a paragraph describing the uncertainty associated with several assumptions involved in this work.*

Reply*:* Please see the reply above about the uncertainty analysis.

- *Page 10007, 1st paragraph: This result essentially resembles the finding of several previous studies which showed based on the RT simulations that the TOA forcing is a strong function of the surface albedo. Over the Arabian Sea, dust frequently over- lies low-level clouds during the Indian summer monsoon. However, these clouds are patchy, broken, and shallow and therefore less efficient in reflecting sunlight. The scattering effects, therefore, dominate over the aerosol absorption which results in negative forcing at TOA. More precisely, the sign and magnitude of DRE for ACA situations is modulated by COD. At the same time, above-cloud AOD is also a co-determinant of the DRE.*

Reply*:* Thank you for these comments that we are largely in agreement with.

Dear Dr. Wilcox,

We'd like to thank you for reviewing our paper. We have carefully considered your comments and suggestions, and revised the manuscript accordingly. Thanks to your comments/suggestions, we felt that the manuscript is significantly improved. Point-to-point replies to your review are listed below.

- *Since the paper provides a quantitative estimate of the radiative effect, I feel the authors are obligated to provide a credible estimate of the uncertainty in the radiative effect. The authors are to be commended for acknowledging at least two important sources of uncertainty: the assumed independent uce of above cloud aerosol optical thickness from the cloud optical thickness below, and the bias error that is suspected in the aerosol optical thickness retrieval. Certainly there are others, some of which can be quantified and some that probably cannot. The best available quantitative estimates of these should be propagated through the analysis and provided with the radiative effect quantities. One important reason to do this is so that estimates of the same quantity based on other techniques can be done. Inevitably, the values for the radiative effect will differ between the different techniques, but the uncertainties at least provide a means of determining whether the differences lie within or outside the estimated uncertainties. There are a few other published estimates and I think the authors should try to compare with them in addition to the Meyer et al. (2013) estimate. Others I am aware of include Costantino and Breon (2013), and Wilcox (2012) – there may be others. Sometimes differences in averaging and domain make a direct comparison to a published value impossible. I think in the case of my own estimate, the number I quote in the abstract of Wilcox (2012), 9.2 +/- 6.6 W mˆ-2, is comparable to the 6.63 W mˆ-2 reported on the last line of page 10004 of the current paper. So in this case the numbers differ, but only within the admittedly broad range of uncertainty I estimated in my paper.*

Reply: Yes, indeed uncertainty analysis should be part of our method and this paper. In the revised manuscript, we added a new Section 3.4 to discuss how to estimate the impact of CALIOP AOD uncertainty on DRE computation.

Once the nature and size of the uncertainty in the input AOD (or/and COD for that matter) are known, it is trivial to apply an uncertainty analysis on our method. We simply perturb the PDF of AOD or COD according to the estimated uncertainties and then compute the DRE based on perturbed PDF. Note that the uncertainty analysis in our method (i.e., based on Eq. 2) requires **no** additional radiative transfer computations because both the perturbed and original DRE can be computed using the same integral, with only the weightings being different. Please see Section 3.4 of the revised manuscript, as well as our replies to the other two reviewers, for details on uncertainty estimation

- *The paper notes that it is assumed that the cloud optical thickness beneath an aerosol layer is independent of the aerosol optical thickness above the cloud. Although I am on the record arguing that they are related (Wilcox 2010), at least over the South- east Atlantic Ocean, I think the authors may make the assumption for the purposes of advancing the methodology. I suspect that the conditions under which above-cloud aerosol will affect cloud optical thickness through a cloud response to aerosol radiative effects is possibly a limited fraction of all cases of detectable aerosol over cloud, although that is merely a guess – it is not clear that the assertion can be properly evaluated globally with the available data. I suggest that the authors clearly restate this assumption in the "summary and discussion" section of the paper.*

Reply: The uncertainty associated with the assumption that above-cloud AOD and below-aerosol COD are independent is apparently small (<5%), as evidenced by the close agreement between our method and the pixel-by-pixel computation in which the potential correlation between above-cloud AOD and below-aerosol COD is fully accounted for.

Nevertheless, we want to emphasize that our assumption is that the ***instantaneous*** above-cloud AOD and below-aerosol COD are independent *at* ***sub-grid scale***. This assumption does **not** contradict the possibility that above-cloud AOD and below-aerosol COD could be correlated at longer temporal (e.g., seasonal) and/or larger spatial (e.g., regional) scale through the thermodynamic and radiative coupling as suggested in [*Wilcox*, 2010; 2012].

References:

Chand, D., R. Wood, T. L. Anderson, S. K. Satheesh, and R. J. Charlson (2009), Satellite-derived direct radiative effect of aerosols dependent on cloud cover, *Nature Geoscience*, *2*(3), 181–184, doi:10.1038/ngeo437.

de Graaf, M., L. G. Tilstra, P. Wang, and P. Stammes (2012), Retrieval of the aerosol direct radiative effect over clouds from spaceborne spectrometry, *J Geophys Res*, *117*(D7), doi:10.1029/2011JD017160.

Jethva, H., O. Torres, F. Waquet, D. Chand, and Y. Hu (2014), How do A-train sensors intercompare in the retrieval of above-cloud aerosol optical depth? A case study-based assessment, *Geophysical Research Letters*, n/a–n/a, doi:10.1002/2013GL058405.

Jethva, H., O. Torres, L. A. Remer, and P. K. Bhartia (2013), A color ratio method for simultaneous retrieval of aerosol and cloud optical thickness of above-cloud absorbing aerosols from passive sensors: Application to MODIS measurements, *IEEE TRANSACTIONS ON GEOSCIENCE AND REMOTE SENSING*, *51*(7), 3862–3870.

Levy, R. C., L. A. Remer, D. Tanre, S. Mattoo, and Y. J. Kaufman (2009), Algorithm for remote sensing of tropospheric aerosol over dark targets from MODIS: Collections 005 and 051: Revision 2, *MODIS Algorithm Theoretical Basis Document for the MOD04_L2 Product*.

Meyer, K., S. Platnick, L. Oreopoulos, and D. Lee (2013), Estimating the direct radiative effect of absorbing aerosols overlying marine boundary layer clouds in the southeast Atlantic using MODIS and CALIOP, *Journal of Geophysical Research-Atmospheres*, n/a–n/a, doi:10.1002/jgrd.50449.

Min, M., and Z. Zhang (n.d.), **On the influence of cloud fraction diurnal cycle and sub-grid cloud optical thickness variability on all-sky direct aerosol radiative forcing**

, *Journal of Quantitative Spectroscopy and Radiative Transfer*, ((submitted)).

Omar, A. H., D. M. Winker, and J.-G. Won (2004), Aerosol models for the CALIPSO lidar inversion algorithms,, 153–164.

Omar, A. H., D. M. Winker, M. A. Vaughan, Y. Hu, C. R. Trepte, R. A. Ferrare, K.-P. Lee, C. A. Hostetler, C. Kittaka, and R. R. Rogers (2009), The CALIPSO automated aerosol classification and lidar ratio selection algorithm, *Journal of Atmospheric and Oceanic Technology*, *26*(10), 1994–2014.

Torres, O., H. Jethva, and P. K. Bhartia (2012), Retrieval of Aerosol Optical Depth above Clouds from OMI Observations: Sensitivity Analysis and Case Studies, *http://dx.doi.org/10.1175/JAS-D-11-0130.1*, *69*(3), 1037–1053, doi:10.1175/JAS-D-

11-0130.1.

Waquet, F., J. Riedi, L. C. Labonnote, P. Goloub, B. Cairns, J. L. Deuzé, and D. Tanre (2009), Aerosol Remote Sensing over Clouds Using A-Train Observations, *J Atmosph Sci*, *66*(8), 2468–2480, doi:10.1175/2009JAS3026.1.

Wilcox, E. M. (2010), Stratocumulus cloud thickening beneath layers of absorbing smoke aerosol, *Atmospheric Chemistry and Physics*, *10*(23), 11769–11777, doi:10.5194/acp-10-11769-2010.

Wilcox, E. M. (2012), Direct and semi-direct radiative forcing of smoke aerosols over clouds, *Atmospheric Chemistry and Physics*, *12*(1), 139–149, doi:10.5194/acp-12-139-2012.

Wood, R., C. S. Bretherton, and D. L. Hartmann (2002), Diurnal cycle of liquid water path over the subtropical and tropical oceans, *Geophysical Research Letters*, *29*(23), 2092–, doi:10.1029/2002GL015371.

A novel method for estimating shortwave direct radiative effect of above-cloud aerosols using CALIOP and MODIS data

Zhibo Zhang[*,1,2], Kerry Meyer[3,4], Steven Platnick[4], Lazaros Oreopoulos[4], Dongmin Lee[4,5] and Hongbin Yu[4,6]

1. Department of Physics, University of Maryland, Baltimore County (UMBC), Baltimore, MD, USA
2. Joint Center Earth Systems & Technology (JCET), UMBC, Baltimore, MD, USA
3. Goddard Earth Sciences Technology and Research (GESTAR), Universities Space Research Association, Columbia, MD, USA
4. NASA Goddard Space Flight Center, Greenbelt, Maryland, USA
5. Goddard Earth Sciences Technology and Research (GESTAR), Morgan State University, Baltimore, MD, USA
6. Earth System Science Interdisciplinary Center, University of Maryland, College Park, MD, USA

- Corresponding author at: Department of Physics, UMBC, Baltimore, MD, 21250, USA, Tel: 410-455-6315,

  Email: Zhibo.Zhang@umbc.edu (Z. Zhang)

Revised for AMT

Abstract

This paper describes an efficient and unique method for computing the shortwave direct radiative effect (DRE) of aerosol residing above low-level liquid-phase clouds using CALIOP and MODIS data. It addresses the overlap of aerosol and cloud rigorously by utilizing the joint histogram of cloud optical depth and cloud top pressure while also accounting for sub-grid-scale variations of aerosols. The method is computationally efficient because of its use of grid-level cloud and aerosol statistics, instead of pixel-level products, and a pre-computed look-up table based on radiative transfer calculations. We verify that for smoke and polluted dust over the southeast Atlantic Ocean the method yields a seasonal mean *instantaneous* (approximately 1:30PM local time) shortwave DRE of above cloud aerosol (ACA) that generally agrees with more rigorous pixel-level computation within 4%. We also estimate the impact of potential CALIOP aerosol optical depth (AOD) retrieval bias of ACA on DRE. We find that the regional and seasonal mean *instantaneous* DRE of ACA over southeast Atlantic Ocean would increase, from the original value of 6.4 W m^{-2} based on operational CALIOP AOD to 9.6 W m^{-2} if CALIOP AOD retrievals are biased low by a factor of 1.5 (Meyer et al., 2013) and further to 30.9 W m^{-2} if CALIOP AOD retrievals are biased low by a factor of 5 as suggested in (Jethva et al., 2014). In contrast, the instantaneous ACA radiative forcing efficiency (RFE) remains relatively invariant in all cases at about 53 W m^{-2} AOD^{-1}, suggesting a near linear relation between the instantaneous RFE and AOD. We also compute the annual mean instantaneous shortwave DRE of light-absorbing aerosols (i.e., smoke and polluted dust) over global oceans based on 4 years of CALIOP and MODIS data. We find that given an above-cloud aerosol type the optical depth of the underlying clouds plays a larger role than above-cloud AOD in the variability of the annual mean shortwave DRE

1 of above-cloud light-absorbing aerosol. While we demonstrate our method using
2 CALIOP and MODIS data, it can also be extended to other satellite data sets.
3

1. Introduction

The shortwave direct radiative effect (DRE) of aerosols at the top of the atmosphere (TOA) is strongly dependent on the reflectance of the underlying surface. Over dark surfaces (e.g. ocean, vegetated land), the scattering effect of aerosols is generally dominant, leading to negative DRE (i.e., cooling) at TOA (Yu et al., 2006). In contrast, when light-absorbing aerosols occur above clouds or other bright surfaces (such as snow, ice, desert), aerosol absorption is significantly amplified by cloud or surface reflection, offsetting or even exceeding the scattering effect of the aerosol, leading to a less negative or even positive (i.e., warming) TOA DRE (Abel et al., 2005; Keil and Haywood, 2003; Twomey, 1977). Therefore, in order to understand the full complexity of aerosol radiative effects on climate, it is important to quantify the DRE under both clear-sky and cloudy-sky conditions. The DRE of aerosols in clear-sky regions has been extensively studied and is relatively well constrained based on advanced satellite remote sensing measurements acquired in the last decade (Yu et al., 2006). However, currently model simulations shows a large inter-model spread in cloudy-sky DRE (Schulz et al., 2006), which results from inter-model differences in both aerosol and cloud properties (Schulz et al., 2006; Stier et al., 2013). Therefore, there is a clear need for an observational constraint on the DRE of above-cloud aerosol (ACA).

Recent advances in satellite remote sensing techniques have provided an unprecedented opportunity for studying the DRE of ACA. In particular, the availability of measurements from the space-borne Cloud-Aerosol Lidar with Orthogonal Polarization (CALIOP) sensor onboard NASA's Cloud-Aerosol Lidar and Infrared Pathfinder

Satellite Observations (CALIPSO) satellite has provided a revolutionary global view of the vertical distribution of aerosols and clouds (e.g., Winker et al., 2013). Using CALIOP aerosol and cloud layer products, Devasthale and Thomas (2011) found frequent occurrences of aerosols residing above low-level clouds in several regions of the globe. In particular, they found a high frequency of smoke occurrence over low clouds in the southeast Atlantic, western coasts of South America (e.g., Columbia, Ecuador, and Peru) and southern Asia. These authors also found a high frequency of natural and polluted dust aerosols overlapping low clouds off the western coasts of Saharan Africa in boreal summer and over boundary layer clouds in the eastern coast of China in boreal spring (see Fig. 3 of Devasthale and Thomas, 2011).

CALIOP measurements of ACA properties, in combination with satellite cloud products from, for example, the Moderate Resolution Imaging Spectroradiometer (MODIS), have been used in several recent studies to derive the DRE of ACA with radiative transfer simulations (e.g., Chand et al., 2009; Costantino and Bréon, 2013b; Meyer et al., 2013; Oikawa et al., 2013). (Chand et al., 2009) used CALIOP above-cloud AOD retrievals (Chand et al., 2008) and Terra-MODIS cloud products, both aggregated to 5º gridded monthly means, to calculate the radiative effects of smoke transported above the low-level stratocumulus deck in the southeastern Atlantic. The spatial-temporal aggregation of both CALIOP and MODIS data to coarse gridded monthly means obscures the potential influence of cloud and aerosol variability on the DRE. In particular, using grid box mean cloud optical depth for DRE calculation might lead to biases in DRE due to the plane-parallel albedo bias (Oreopoulos et al., 2007). Moreover, the MODIS level-3 aggregation algorithm samples all liquid water clouds, regardless of whether or

not there is an aerosol layer above cloud. As a result, the total population of liquid water clouds in the MODIS level-3 products (daily or monthly) may be significantly different from that of below-aerosol-only cloud population. Therefore, using level-3 MODIS products without distinguishing below-aerosol-only from total cloud population can potentially lead to significant errors. The problem could be further complicated by biases in MODIS cloud retrievals associated with the presence of overlying light-absorbing aerosols. When a cloud-pixel is contaminated by overlying light-absorbing aerosols the MODIS cloud optical depth (COD) retrieval is generally biased low (e.g., Coddington et al., 2010; Haywood et al., 2004; Jethva et al., 2013; Wilcox, 2010), an effect not considered in most previous studies (e.g., Chand et al., 2009; Costantino and Bréon, 2013b; Oikawa et al., 2013). Most recently however, (Meyer et al., 2013) collocated CALIOP above-cloud AOD and Aqua-MODIS cloud properties at the pixel level, and the DRE was then computed at these individual collocated pixels. They found that correcting the MODIS COD bias due to ACA contamination leads to a more positive ACA DRE. Such rigorous collocation has obvious advantages as it takes into account the sub-grid variability of clouds and aerosols, but is on the other hand computationally expensive since it requires large amounts of pixel-level data that make global scale and multiyear studies challenging.

The objective of this paper is to describe a novel method for computing the DRE of ACA. This method attempts to balance the need for computational efficiency with the need for rigorous treatment of aerosol-cloud overlap and small-scale variability of aerosol and clouds. Our method has several unique features: 1) it takes sub-grid scale cloud and aerosol variation into account in DRE computations; 2) it treats the overlap of aerosol and

cloud rigorously by utilizing the joint histogram of COD and cloud top pressure (CTP) in the MODIS level-3 product; 3) it is computationally efficient because of the use of a pre-computed look-up table of ACA DRE.

In the following sections, we briefly introduce the CALIOP and MODIS data used (Section 2), describe the key assumptions and features of the novel method (Section 3), validate it through comparison with pixel-level computations as in (Meyer et al., 2013) (Section 4), and conclude with a summary and discussion (Section 5).

2. Satellite Data

In (Meyer et al., 2013), the MODIS level-2 cloud product is collocated with CALIOP level-2 aerosol product for every pixel along the CALIOP track and the computation of instantaneous DRE is performed pixel-by-pixel. Then, the pixel-level DRE results are aggregated on a latitude-longitude grid for climatological study. If only the grid-level DRE is of interest, the pixel-by-pixel computation of DRE may not be efficient because of redundant computations. For example, if two pixels with the same above-cloud AOD and below-cloud COD occur within the same grid-box, they evidently have the same ACA DRE, but the radiative transfer computation is nevertheless performed twice in the pixel-by-pixel method. As shown in Section 3, a more efficient way is to compute the DRE statistically using the probability density function (PDF) of above-cloud AOD and below-cloud COD. In this study, we use the CALIOP level-2 aerosol and cloud layer product (V3.01) to derive the statistics of ACA properties and the MODIS level-3 daily cloud product for cloud property statistics. It important to note that our method is not limited to CALIOP and MODIS products, but also applicable to other satellite data sets, such as above-cloud aerosol retrievals from POLDER (POLarization and Directionality

of the Earth's Reflectances) (Waquet et al., 2009) and OMI (Ozone Monitoring Instrument)(Torres et al., 2012), and cloud retrievals from ISCCP (International Satellite Cloud Climatology Project) (Rossow and Schiffer, 1999) and SEVIRI (Spinning Enhanced Visible and Infrared Imager)(Schulz et al., 2009).

2.1. CALIOP level-2 aerosol and cloud layer products

Since its launch in 2006, the space-borne lidar CALIOP has continuously acquired, with near global (albeit instantaneously sparse) coverage, attenuated backscatter measurements at 532 nm and 1064 nm, including linear depolarization information at 532nm (Winker et al., 2009). The CALIOP level-2 retrieval algorithm consists of several steps. First, a "feature finder" algorithm and cloud-aerosol discrimination (CAD) algorithm are used to detect aerosol and cloud layers, and record their top and bottom heights and layer integrated properties (Vaughan et al., 2009). Second, the detected aerosol layers are further classified into six sub-types (i.e., polluted continental, biomass burning, desert dust, polluted dust, clean continental and marine) (Omar et al., 2009) and the detected cloud layers are assigned different thermodynamic phases (Hu et al., 2007a) based on the observed backscatter, color ratio and depolarization ratio. Third, *a priori* lidar ratios, pre-selected based on aerosol sub-type and cloud phase, are used to derive the extinction of an aerosol or cloud layer from the attenuated backscatter profile (Young and Vaughan, 2008).

In this study, we use CALIOP level-2 version 3.01 aerosol and cloud layer products at a nominal 5 km horizontal resolution (i.e., CAL_LID_L2_05kmALay and CAL_LID_L2_05kmCLay) for aerosol-cloud overlap detection, and for information on aerosol layer properties, including type, aerosol optical depth (AOD), and layer top and

bottom height. In addition to physical properties, the CALIOP layer products also provide various metrics and flags on data quality assurance. These include CAD score (Liu et al., 2009), horizontal averaging scale, extinction quality control (QC) flag, and estimated uncertainty of layer AOD. In this study, we apply these metrics following best practices provided by the CALIPSO science team to screen for reliable retrievals (e.g., Winker et al., 2013) (see Table 1).

It should be noted here that the current version of CALIOP operational aerosol retrieval algorithm (V3.01) appears to significantly underestimate the AOD of above-cloud aerosol layer according to recent studies (Jethva et al., 2014; Liu et al., 2013; Waquet et al., 2013b). The main reason is that after strong attenuation by the upper part of an aerosol layer, the 532 nm attenuated backscatter of the lower part of aerosol layer is often too small. As a result, the current CALIOP feature detection algorithm often cannot resolve the full depth of the aerosol layer, leading to low biases in retrieved AOD (Jethva et al., 2014; Liu et al., 2013). At the moment, the CALIOP operational team is investigating the possibility of using the algorithm described in (Chand et al., 2008; Hu et al., 2007b) for ACA retrievals (Liu et al., 2013). This alternate method utilizes the reflected lidar signal from the bright cloud layer underneath to derive the two-way transmittance and thereby the AOD of the ACA layer. Because the backscatter of a cloud layer is usually very strong, the two-way transmittance method is less affected by the strong attenuation of the ACA layer and is therefore expected to alleviate the aforementioned problem. Lidar based AOD retrievals are also known to suffer from other issues, such as the background solar noise during daytime. These issues are beyond the scope of this study, but are nevertheless discussed in the uncertainty analysis of Section

3.4.

In addition to retrieval errors and uncertainties, another limitation of CALIOP data is the small sampling rate (i.e., only along track). In order to compute the DRE of ACA over a given latitude-longitude grid box, we assume that the aerosol property statistics retrieved by CALIOP along its narrow track represent the statistics over the whole grid box, i.e., that AOD PDFs are identical. This assumption constitutes an uncertainty in our DRE computation. Due to a lack of satellite-based wide-swath ACA datasets, however, it is difficult to determine the size of this uncertainty. Recently, several novel methods have been developed to retrieve ACA properties from passive sensor observations (Jethva et al., 2013; Torres et al., 2012; Waquet et al., 2009; 2013a), which will help improve our understanding of the sub-grid ACA variability when they become available to public.

Finally, we emphasize two more points. First, none of the aforementioned problems with CALIOP data, e.g., smoke AOD bias, retrieval uncertainties, and small sampling rate, are unique to our method. Any method that uses CALIOP data faces the same challenges. Second, our method is not limited only to CALIOP data. We choose to use CALIOP product in this study solely because it is the only publically available ACA product at the moment. Our method can also be applied to other ACA retrieval products, based on for example, POLDER (Waquet et al., 2009), MODIS (Jethva et al., 2013), OMI (Torres et al., 2012) observations when they become available to public. In fact, as discussed later, the advantage of our method in terms of computational efficiency is even greater when applied on retrievals from passive sensors.

2.2. MODIS daily level-3 cloud property product

This study computes the grid-level ACA DRE using the statistics of aerosol and cloud properties, instead of pixel-by-pixel computation as in (Meyer et al., 2013). We use the Collection 5 (C5) Aqua MODIS level-3 *Daily* gridded Atmosphere product MYD08_D3 for the statistics of cloud properties and other parameters, such as solar zenith angle, needed for ACA DRE computations.

The MODIS level-3 (i.e., grid-level) product contains statistics computed from a set of level-2 (i.e., pixel-level) MODIS granules. As summarized in (Platnick et al., 2003), the operational level-2 MODIS cloud product provides cloud masking (Ackerman et al., 1998), cloud top height retrieval based on CO_2 slicing or the infrared window method (Menzel et al., 1983), cloud top thermodynamic phase determination (Menzel et al., 2006), and cloud optical and microphysical property retrieval based on the bi-spectral solar reflectance method (Nakajima and King, 1990). In addition to these cloud parameters, the level-2 products also provide pixel-level runtime Quality Assessment (QA) information, which includes product quality as well as processing path information. All MODIS level-2 atmosphere products, including the cloud, aerosol and water vapor products, are aggregated to 1° spatial resolution on a daily (product name MYD08_D3 for Aqua MODIS), eight-day (MYD08_E3), and monthly (MYD08_E3) basis. Aggregations include a variety of scalar statistical information (mean, standard deviation, max/min occurrences) and histograms (marginal and joint). A particularly useful level-3 cloud product for this study is the daily joint histogram of COD vs. CTP, derived using daily counts of successful daytime level-2 pixel retrievals that fall into each joint COD-CTP bin. Eleven COD bins, ranging from 0 to 100, and 13 CTP bins, ranging from 200 to

1000 mb, comprise the histogram. As discussed below, the COD-CTP joint histogram allows for identification of the portion of the cloud population that lies beneath the aerosol layer found by CALIOP, as well as the corresponding COD probability distribution needed for DRE estimation. In addition to the COD-CTP joint histogram, we also use the gridded mean solar and sensor zenith angles for calculating DRE and correcting the COD bias due to the presence of ACA.

It should be noted that the level-3 daily product MYD08_D3 contains statistics computed from a set of level-2 MODIS granules that theoretically span a 24-hour interval (Hubanks et al., 2008). However, for cloud parameters retrieved only during daytime, such as COD and cloud droplet effective radius (CER), only daytime level-2 files are used to compute the level-3 daily statistics. These are called *daytime only* SDSs (Scientific Data Sets) in level-3 products. Strictly speaking, the *daytime only* SDSs of only those 1° gridcells between approximately 23° N and 23° S come from a single MODIS overpass. The tropical southeast Atlantic region, where transported smoke aerosols are often observed above low-level stratocumulus clouds, is well within this range (about 10° N~30° S see Figure 3). The COD statistics in MYD08_D3 product for this region are therefore derived from a single Aqua-MODIS overpass that can be collocated with CALIOP observations (see Section 3.1 for details on collocation). The DRE computed based on the collocated dataset is therefore *instantaneous* DRE at Aqua crossing time (1:30PM) that are directly comparable to the pixel-by-pixel results in (Meyer et al., 2013). Poleward of 23°, MYD08_D3 statistics are derived from averaging several overlapping orbits approximately 100 minutes apart (Hubanks et al., 2008). As a result, strictly speaking the DRE computed for mid and high latitude regions based on

MYD08_D3 data is not *instantaneous* DRE. We emphasize that this is not a limitation of our method, but an inherent characteristic of the MODIS level-3 product.

3. Methodology

3.1. Theoretical basis

As in previous investigations (e.g., Chand et al., 2008; 2009; Costantino and Bréon, 2013b; Meyer et al., 2013), we focus on the simplest case of overlapping aerosol and cloud, i.e., a single layer of aerosol overlying a single layer of low-level liquid-phase clouds, which is commonly observed in many regions of the globe (Devasthale and Thomas, 2011). More complex situations certainly exist, such as an aerosol layer located in between high and low cloud, or an aerosol layer overlying multiple layers of clouds. However, identification of such situations are either beyond the detection capabilities of CALIOP or relatively rare (Devasthale and Thomas, 2011). As such, they are not considered here and left for future research.

To illustrate the theoretical foundation of the method, consider the schematic example in Figure 1. For a given grid box (e.g., 1°×1° in case of MODIS level-3 data), the gridded mean *instantaneous* broadband shortwave DRE ($\langle DRE \rangle_{ACA}$) averaged over all ACA pixels within the grid box is given by:

$$\langle DRE \rangle_{ACA} = \int_0^\infty \int_0^\infty DRE(\tau_c, \tau_a) p(\tau_c, \tau_a) d\tau_c d\tau_a, \quad (1)$$

where $p(\tau_c, \tau_a)$ is the joint probability density function (PDF) of the above-cloud AOD at 532 nm (τ_a) and below-aerosol COD (τ_c) of ACA pixels. We note that, in addition to τ_a, DRE also depends on the spectral variation of aerosol and cloud optical depth, spectral single scattering albedo and asymmetry factor, wavelength dependencies not

explicitly shown in this equation. These properties are computed using a Mie scattering code (Wiscombe, 1980) based on the aerosol model described in (Meyer et al., 2013). The dependencies on solar zenith angle, surface reflectance, cloud particle effective radius, and atmospheric profile are also omitted from the equation; solar zenith angle and surface reflectance are expected to have only minor variation within the grid box, while the impact of cloud particle effective radius and atmospheric profile on shortwave DRE is relatively small. Since $p(\tau_c,\tau_a)$ describes the covariation of aerosols and clouds for the ACA pixels, it should ideally be derived from collocated CALIOP aerosol and MODIS cloud retrievals at pixel level as in (Meyer et al., 2013). However, this requires large amounts of pixel-level data. Therefore, pixel-level collocation and radiative transfer simulation are too computationally expensive and cumbersome for multiyear global studies.

A key assumption in our method, which allows us to avoid tedious pixel-level collocation, is that the *sub-grid level instantaneous* spatial distribution of above-cloud AOD is statistically independent from the *sub-grid level instantaneous* spatial distribution of below-aerosol COD. Under this assumption, $p(\tau_c,\tau_a)=p(\tau_c)\cdot p(\tau_a)$ and Eq. (1) reduces to:

$$\left\langle DRE\right\rangle_{ACA}=\int_0^\infty\left[\int_0^\infty DRE(\tau_c,\tau_a)p(\tau_c)d\tau_c\right]p(\tau_a)d\tau_a, \qquad (2)$$

where $p(\tau_c)$ and $p(\tau_a)$ are the PDF of *instantaneous* below-aerosol COD τ_c and above-cloud AOD τ_a, respectively, of ACA pixels. The advantage of Eq. (2) is that it allows $p(\tau_c)$ and $p(\tau_a)$ to be derived separately and independently. This assumption is

reasonable considering that transported ACAs and low-level boundary layer clouds are usually well separated vertically (Devasthale and Thomas, 2011) and controlled by different meteorological conditions. The potential coupling between the two is that overlying absorbing aerosols could influence the evolution of clouds through changing atmospheric stratification (Wilcox, 2010). However, a recent observational study (Costantino and Bréon, 2013a) found no correlation between above-cloud AOD and below-aerosol COD, although correlations are found between AOD and cloud droplet effect radius, as well as liquid water path. Moreover, it is important to stress that our assumption is that the *instantaneous* above-cloud AOD and below-aerosol COD are independent *at sub-grid scale*. This assumption does not rule out the possibility that AOD and COD could be correlated at longer temporal (e.g., seasonal) and/or larger spatial (e.g., regional) scale through the thermodynamic and radiative coupling (Wilcox, 2010; 2012). Finally, as shown in section 4, when we compare the DRE derived from pixel-level collocation (i.e., based on Eq. (1)) with that from independent sampling of $p(\tau_c)$ and $p(\tau_a)$ (i.e., based on Eq. (2)) the agreement is very good.

In our method, the PDF of above-cloud AOD $p(\tau_a)$ is derived from the CALIOP 5km aerosol and cloud layer products through the following steps: 1) for each 5km CALIOP profile that falls within a given latitude-longitude grid box, we first search for an aerosol layer; 2) if an aerosol layer is detected and the quality metrics pass the quality assurance criteria summarized in Table 1, we then proceed to check for the presence of an underlying liquid-phase cloud layer within the profile using the CALIOP cloud layer product; 3) if a cloud layer is present, the AOD of the aerosol layer is recorded for the

derivation of the $p(\tau_a)$ of the grid box. The bottom height of the aerosol layer is also recorded to derive the grid mean aerosol layer bottom height. Once all of the CALIOP profiles within the grid box are processed, we obtain the PDF of the above-cloud AOD $p(\tau_a)$ and the mean aerosol layer bottom pressure $\langle P_{bottom} \rangle$.

As schematically illustrated in Figure 1, the PDF of below-aerosol COD $p(\tau_c)$ is derived from the joint histogram of cloud optical depth and cloud top pressure (COD-CTP joint histogram) in the MODIS daily level-3 product, using the grid mean aerosol layer bottom pressure $\langle P_{bottom} \rangle$ derived above. For a given grid box, we first identify the population of liquid-phase clouds below the pressure level $\langle P_{bottom} \rangle$. This subset, together with the AOD PDF $p(\tau_a)$, is then used to calculate DRE according to Eq. (2).

In this study, we focus on the computation of instantaneous DRE. To obtain diurnally averaged DRE, technically speaking one would simply need to integrate over time the instantaneous DRE. However, it is important to note that, in addition to diurnal variation of solar zenith angle, aerosol and cloud properties may also have significant diurnal cycles. In fact, it is known that the low cloud fraction over stratocumulus regimes, such as the South East Atlantic region, have a strong diurnal cycle (15~35% of diurnal mean value) driven by cloud solar absorption(Wood et al., 2002). A recent study by (Min and Zhang, n.d.) indicates that using a constant cloud fraction based on Aqua-MODIS observations tends to result in significantly underestimated diurnal mean DRE even if the diurnal variation of solar zenith angle is considered in the computation. Therefore, the diurnal variation of cloud properties is an important factor to consider in the inter-

comparison of DRE computations based on different datasets and inter-comparison between observational study and modeling results.

3.2. DRE Look-up Tables

To speed up calculations, we use pre-computed aerosol-type specific look-up-tables (LUTs), instead of online radiative transfer computation, when deriving the DRE of ACA. The concept of our LUTs is somewhat similar to the "radiative kernels" described in (Hartmann et al., 2001) and (Zelinka et al., 2012) for computing cloud radiative feedbacks. The LUT for each aerosol type consists of DREs at both TOA and surface (not used in this study) for various combinations of AOD, COD, CTP and solar zenith conditions. As such, once the aerosol type and AOD are known from CALIOP and COD, CTP and solar zenith angle are known from MODIS, the corresponding DRE can be obtained through LUT interpolation. Note that the CALIOP only provides AOD at lidar wavelengths (e.g., 532 nm and 1064 nm) for each aerosol type. Therefore, radiative transfer model-appropriate narrowband aerosol scattering properties, namely AOD, single-scattering albedo and asymmetry factor, are needed for the development of the LUT. The current version of LUT focuses on light-absorbing aerosols (e.g., smoke and polluted dust). In order to validate our method with more rigorous pixel-level computations, we adopt the narrowband aerosol optical properties of (Meyer et al., 2013), who used the same radiative transfer code, in the computation of the current LUT. The aerosol model in (Meyer et al., 2013) is extended from an absorbing aerosol model developed for the MODIS Collection 5 Aerosol Product (MOD04) (see Table 4 of Levy et al., 2009). The MOD04 aerosol models define aerosol size distributions and refractive indices based solely on prescribed AOD at 550 nm (MODIS band 4; note that the

absorbing aerosol model used here assumes a constant index of refraction, 1.51–0.02i, at all wavelengths). At AOD=0.5 (550 nm), the single-scattering albedo of this model is about 0.9 over the visible spectral region (see Figure 7 of Meyer et al., 2013), which is in the range of previously reported values (e.g., Keil and Haywood, 2003; Myhre et al., 2003). The current AOD bins (at 550 nm) in the LUT range from 0.05 to 1.5, which covers most of the above-cloud AOD observed by CALIOP. The current COD bins, logarithmically spaced, range from 0.1 to 300. Following the MODIS level-3 data, the thirteen CTP bins range from 1000mb to 200mb. The solar zenith angle bins range from 0 to 80 degree. Radiative transfer computations are carried out using the RRTM-SW model (Clough et al., 2005; Iacono et al., 2008). Lambertian ocean surface reflectance is set to 5%. Cloud droplet effective radius is fixed at 15 μm, which is close to the global mean value over oceans observed by MODIS (King et al., 2013). This value of effective radius is also used to convert the MODIS visible COD to liquid water path used as input to RRTM-SW. Liquid cloud optical properties are calculated internally by RRTM. For atmospheric profiles of water vapor and temperature, we use NCEP R1 reanalysis data (Kistler et al., 2001) averaged both zonally and annually. Our sensitivity tests indicate that the shortwave DRE of ACA is largely insensitive to cloud effective radius or atmospheric profiles.

3.3. Cloud Optical Depth Correction

As noted in previous studies (Coddington et al., 2010; e.g., Haywood et al., 2004), when a cloudy MODIS pixel is contaminated by overlying light-absorbing aerosols the COD retrieval is generally biased low. We have developed a fast COD correction scheme to account for the COD retrieval bias due to ACA in our DRE computation, which is

illustrated in Figure 2. This scheme requires both the cloud reflectance LUT for clouds without ACA, for which we use the MODIS operational LUT, and clouds with ACA, for which we use the one developed by Meyer et al. (2013). In the operational MODIS retrieval, the reflectance LUT of cloud without ACA is used to interpret the reflectance of all clouds, including those affected by ACA. Based on this fact, we first infer the "observed" cloud reflectance (after atmospheric correction) by interpolating the reflectance LUT of cloud without ACA corresponding to the biased COD. Then, we use the "observed" cloud reflectance and ACA-affected LUT (derived based on CALIOP AOD) to determine the corrected COD. This COD correction process is performed for every combination of COD bin in $p(\tau_c)$ and AOD bin in $p(\tau_a)$. In the final step we resample the corrected CODs to obtain the corrected $p(\tau_c)$.

It should be noted that because different aerosol type may have different impact on MODIS COD retrievals, the above COD correction process is aerosol-type dependent. In this study, we use light-absorbing aerosols as example to illustrate our method and for validation purposes we use the aerosol model developed by (Meyer et al., 2013) for the development of LUTs for DRE computation and COD correction. However, the LUTs can be easily extended to other aerosol models. In fact, as part of ongoing research, we are extending our LUTs to include all six operational CALIOP aerosol models as described in (Omar et al., 2009).

3.4. Uncertainty Analysis

Several recent studies suggest that the current operational CALIOP product tends to underestimate the above-cloud AOD. Meyer et al. (2013) found that the daytime CALIOP AOD retrievals are systematically smaller than the nighttime retrievals,

probably due to the daytime solar background issue. In the light of this finding, Meyer et al. (2013) increased the CALIOP AOD retrievals by a factor of 1.5 to account for the impact of potential AOD bias on DRE of ACA. A more recent case study by (Jethva et al., 2014) suggests that CALIOP ACA AOD retrievals are biased low by a factor of 5 or even more compared with other retrievals, although the generality of this finding needs to be further tested with larger samples. While a rigorous analysis uncertainty analysis of CALIOP AOD product is beyond the scope of this study, it is nevertheless reasonable to assume that the current CALIOP retrievals provide a lower limit to the ACA AOD. In the uncertainty analysis presented in the next section, we carry out two sensitivity tests to estimate the potential impacts of CALIOP AOD bias on DRE computation. We multiply CALIOP AOD values by a factor of 1.5 in the first test following (Meyer et al., 2013) and by a factor of 5 in the second as suggested in (Jethva et al., 2014).

Once the magnitude of the uncertainties in the input data is prescribed, the consequential impact on DRE can be easily estimated in our method as follows. First, in addition to the $p(\tau_a)$ based on the original CALIOP data, we also derive the perturbed PDF $\tilde{p}(\tau_a)$ by perturbing the original data according to pre-defined uncertainties (i.e., by increasing the original values by a factor of 1.5 or 5). Then, the impact of input uncertainty on ACA DRE can be estimated by comparing the DREs computed with the original vs. perturbed PDF (i.e., $\langle DRE \rangle_{ACA}$ vs. $\langle \widetilde{DRE} \rangle_{ACA}$). Note that $\langle DRE \rangle_{ACA}$ and $\langle \widetilde{DRE} \rangle_{ACA}$ can be obtained in a single computation because they both represent integrals over $DRE(\tau_c, \tau_a)$, only with different weights. In this regard, our method is much more

efficient than the pixel-by-pixel method, in which uncertainty must be estimated by perturbing individual pixels.

4. Implementation and validation of new DRE estimation scheme

Each year during austral winter, dry season biomass burning activities throughout southern Africa inject large amounts of smoke into the troposphere (Eck et al., 2003; Ichoku et al., 2003; Myhre et al., 2003). Prevailing easterly winds during this season often transport the smoke westward off the continent, over the ocean, where extensive marine boundary layer clouds persist for most of the year. Under the descending branch of the Hadley cell, the air mass above the boundary layer is quite dry. Due to the lack of efficient wet scavenging, the transported aerosol layers can remain suspended in the atmosphere for days, creating a near-persistent smoke layer above the stratocumulus deck over the southeastern Atlantic Ocean (Chand et al., 2009; Devasthale and Thomas, 2011; Keil and Haywood, 2003; Wilcox, 2010).

To validate our method, we have compared the DRE of above-cloud light-absorbing aerosols in this region with pixel-level computations from (Meyer et al., 2013). Figure 3a shows the seasonal mean (August/September 2007-2011) instantaneous TOA DRE of above-cloud smoke and polluted dust based on the pixel-level computations from (Meyer et al., 2013). Figure 3b shows the corresponding instantaneous TOA aerosol radiative forcing efficiency (RFE) defined as the DRE per unit AOD. The DRE and RFE results computed using our method described in the previous section are shown in Figure 3c and Figure 3d, respectively. Evidently, both DRE and RFE computed using our new method agree closely with the pixel-level computations. Figure 4 shows the meridional mean DRE and RFE for the region using the results in Figure 3. Not surprisingly, the outcomes

of the two methods are almost identical. Note that the CODs used in the computations for Figure 3 and Figure 4 are directly from the MODIS products without COD correction. We have also compared the DRE and RFE from the two methods using the corrected COD and achieved again very good agreement (not shown because of close resemblance to Figure 3 and Figure 4). The seasonal and regional mean DRE and RFE, based on the corrected COD, from the pixel-level computation method in (Meyer et al., 2013) are 6.6 W m^{-2} and 56 W m^{-2} AOD^{-1}, respectively (see Table 2). The corresponding values from our new method are 6.4 W m^{-2} and 53.8 W m^{-2} AOD^{-1}, respectively.

As previously mentioned, to estimate potential bias in CALIOP ACA AOD retrieval on our DRE computation, we carried out two sensitivity tests. We increased CALIOP AOD values by a factor of 1.5 in one test following (Meyer et al., 2013) (hereafter refered to as "x1.5 test") and by a factor of 5 in another as suggested in (Jethva et al., 2014) ("x5.0 test" hereafter). In both cases, we corrected the MODIS COD retrievals based on the scaled AOD. The regional and seasonal mean DRE of ACA increases, from the original value of 6.4 W m^{-2} to 9.6 W m^{-2} in the x1.5 test and to 30.9 W m^{-2} in the x5.0 test. We have to note that this is a very rough estimate. Nevertheless, the DRE based on the x1.5 scaling of CALIOP AOD seems to agree reasonably with the value, 9.2±6.6 W m^{-2}, reported in an independent study by Wilcox (Wilcox, 2012). Interestingly, the scaling of AOD has little impact on RFE in both cases (53.1 W m^{-2} AOD^{-1} in the x1.5 case and 51.2 W m^{-2} AOD^{-1} in the x5.0 case), which apparently suggests a near linear relationship between DRE and AOD as also noted in (Meyer et al., 2013) and (Wilcox, 2012) (see his Figure 5).

In summary, as shown clearly in Figure 3, Figure 4 and Table 2, the DRE inferred from our new method agrees very well with the pixel-level computations. Furthermore, the difference between the two methods is much smaller than, for example, the uncertainty associated with CALIOP retrieval biases.

It is worthwhile to clarify again that the results shown in Figure 3 are seasonal mean *instantaneous* DRE at A-Train crossing time (1:30PM local time) based on CALIOP above-cloud AOD and corrected Aqua MODIS below-aerosol COD retrievals. Moreover, the aerosol model described in (Meyer et al., 2013) is used in this study. All these factors should be considered when comparing the results in this study with those in other studies (e.g., Chand et al., 2009; de Graaf et al., 2012; Wilcox, 2012). For example, (Chand et al., 2009) used CALIOP in combination with Terra-MODIS observation to compute the DRE over the South East Atlantic Region. It is known that low-clouds in this region have a strong diurnal cycle driven by solar cloud absorption (Bergman and Salby, 1996; Rozendaal et al., 1995; Wood et al., 2002). As a result the cloud properties observed by Terra-MODIS can be significantly different from those observed by Aqua-MODIS in this region, which could lead to different DRE even if the same method was used.

5. Summary and Discussion

Recent advances in satellite-based remote sensing, in particular the launch of the space-borne lidar CALIOP, have provided an unprecedented opportunity for studying the radiative effects of above-cloud aerosol (ACA). However, the methodologies used in recent studies for computing the ACA DRE appear to be either oversimplified (e.g., Chand et al., 2009; Oikawa et al., 2013) or too cumbersome (e.g., Meyer et al., 2013). This paper describes a novel method recently developed for computing the shortwave

DRE of above-cloud aerosols over ocean. Our method has several unique features compared to previous methods: 1) It takes sub-grid scale cloud and aerosol variation into account in DRE computations, similar to (Meyer et al., 2013); 2) it treats the overlap of aerosol and cloud rigorously by utilizing the joint histogram of COD and CTP in the MODIS level-3 cloud product; 3) it relies on grid-level cloud statistics (i.e., COD-CTP joint histogram), instead of pixel-level products, and utilizes pre-computed look-up tables for ACA DRE computations, making it thus much more efficient than pixel-level computations. As shown in Figure 3, Figure 4 and Table 2, DRE computed using our method agrees well with the pixel-level computations of (Meyer et al., 2013)..

In addition to the Southeast Atlantic region, we have recently begun investigating the DRE of above-cloud light-absorbing aerosols for global ocean. Some preliminary results are shown in Figure 5. We first derived the daily grid-level statistics of above-cloud AOD and below-cloud COD, as well as the corresponding ACA DRE, using the method described above and then aggregated the daily means to annual mean. The temporal aggregation is weighted by the number of ACA pixels in each day during 2007-2010. For example, the annual mean ACA DRE in Figure 5c is aggregated from daily mean based on the following equation:

$$\overline{\langle DRE \rangle_{ACA}} = \frac{\sum_i N_i \cdot \langle DRE_i \rangle_{ACA}}{\sum_i N_i}, \; i\text{=day } 1, 2, 3\ldots \qquad (3)$$

where $\langle DRE_i \rangle_{ACA}$ is the spatially averaged instantaneous ACA DRE in each day averaged over ACA pixels, N_i is the number of ACA pixels in the grid box in each day, and $\overline{\langle DRE \rangle_{ACA}}$ is the annual mean instantaneous ACA DRE shown in Figure 5c. Figure 5a

shows a global map of the annual mean 550 nm AOD of above cloud smoke and polluted dust derived based on 4 years (2007-2010) of CALIOP aerosol and cloud layer products. Similar to (Devasthale and Thomas, 2011), we note several "hotspots" of ACA over the Southeast Atlantic, the East-Central Atlantic off the western coast of Saharan Africa, the Arabian sea, and the North Pacific basin off the coast of eastern Asia. It is interesting to note that the ACA AOD over the east-central Atlantic and Arabian Sea is noticeably larger than that over the southeast Atlantic and North Pacific basin. Figure 5b shows the annual mean below-aerosol COD derived from the MODIS daily level-3 cloud product after the correction of above-cloud AOD contamination using the method described in section 3. A notable feature in the figure is that the below-aerosol COD over the North Pacific basin is significantly larger than that over other ACA regions. Figure 5c shows the annual mean shortwave DRE at TOA aggregated from daily values due to ACA smoke and polluted dust over the global ocean. It is intriguing to see that the DRE of ACA over the North Pacific basin is significantly larger than that over the southeast Atlantic, which is in turn larger than the DRE over the east-central Atlantic and the Arabian Sea. In fact, some negative DREs are observed in the latter two regions. This probably due to the COD of below-aerosol clouds being too thin (Figure 5b) over these regions to have significant radiative effect, so that the radiative effect of ACA is close to that of clear skies (i.e., negative). This is interesting because the above-cloud AOD over these regions is actually larger, while the below–aerosol COD over these regions is smaller, compared to their counterparts over the southeast Atlantic and North Pacific basin. Therefore, the preliminary results seem to suggest that the variability of DRE of ACA is modulated by COD, rather than AOD, although it should be noted that we have focused only on the light-absorbing aerosols, i.e., smoke and polluted dust, and assumed

the same narrowband scattering properties for them as in (Meyer et al., 2013). Further research is needed to study the impact of aerosol type and scattering properties on the temporal-spatial variation of DRE on global scale. Nevertheless, the preliminary results shown Figure 5 clearly demonstrate the usefulness of our new method for global studies.

It should be noted that this study, and previous ones using CALIOP observations (e.g., Chand et al., 2008; Meyer et al., 2013; Oikawa et al., 2013), are limited by the capabilities of CALIOP. Arguably, some aerosols exist above every cloud. However, not all ACA can be detected by CALIOP due to its inherent limitations. Some ACAs are simply too optically thin to be detected, though their radiative effects are also expected to be small. Other situations may also be possible. For example, a confined aerosol layer has larger volume backscatter than a vertically stretched layer, even if the total aerosol amounts are the same, and therefore is more easily detected by CALIOP. Passive sensors, on the other hand, are less affected by the vertical distribution of ACA because they observe column-integrated scattering by aerosols. Recently, several novel techniques have been developed to detect and retrieve ACA properties using passive sensors. (Waquet et al., 2009) developed a method based on multi-angular polarization measurements from POLDER (Polarization and Directionality of the Earth Reflectances) to retrieve the AOD of above-cloud smoke. This method has recently been extended to include both smoke and dust aerosols (Waquet et al., 2013a). Most recently, (Jethva et al., 2013) demonstrated the ability of a color ratio method to retrieve the above-cloud AOD based on MODIS multiple spectral cloud reflectance measurements. A review of the emerging satellite-based observations of above-cloud aerosols can be found in (Yu and Zhang, 2013). The capabilities and limitations of the passive techniques need to be

systematically studied through inter-comparisons and comparison with CALIOP observations, but they may provide a complementary perspective on ACA. Recall that passive imagers have much larger spatial coverage than CALIOP, which makes brute force calculations of the DRE at the pixel level computationally expensive. In this regard, our method satisfies the need for efficiency of ACA DRE computations based on passive imager retrievals.

As a final remark, we would like to point out that the ACA DRE discussed in this study is still a few steps away from the all-sky aerosol radiative effect ($\langle DRE \rangle_{all-sky}$). For a given grid box, the $\langle DRE \rangle_{all-sky}$ can be decomposed into the sum of clear-sky and cloudy-sky DRE:

$$\langle DRE \rangle_{all-sky} = (1 - f_c) \cdot \langle DRE \rangle_{clear} + f_c \cdot f_{ACA} \cdot \langle DRE \rangle_{ACA}, \quad (4)$$

where f_c is the cloud fraction, $\langle DRE \rangle_{clear}$ is the DRE averaged over the clear-sky portion of the grid box, f_{ACA} is the fraction of cloudy pixels with ACA detected by CALIOP or other sensors, and $\langle DRE \rangle_{ACA}$ is the DRE averaged over all ACA containing pixels. It is important to note an implicit assumption made in Eq. (4), that is, when a distinct ACA layer is not detected, the DRE of ACA is zero. Different sensors (or different retrieval algorithms for the same sensor) may have different sensitivities to ACA and therefore provide different estimates of f_{ACA} and $\langle DRE \rangle_{ACA}$. For example, one sensor may only be able to retrieve ACA for optically thick clouds. This sensor would retrieve a larger $\langle DRE \rangle_{ACA}$, but a smaller f_{ACA}, in comparison with another sensor capable of retrieving ACA for all clouds. Therefore, when comparing the ACA or all-sky

DRE estimated based on different instruments or algorithms, it is important to compare both the f_{ACA} and $\langle DRE \rangle_{ACA}$ terms in Eq. (4).

Table 1 Quality control metrics used for screening the CALIOP aerosol layer product.

	Criterion
CAD_score	< −30
Horizontal_averaging	< 20km
Extinction_QC_532	0 or 1
Feature_Optical_Depth_Uncertainty_532	< −99.5

Table 2 Regional and seasonal mean values of instantaneous DRE and RFE based on the pixel-level computation and the new method.

	DRE [W m^{-2}] Bias adjusted (unadjusted)	RFE [W m^{-2} AOD^{-1}] Bias adjusted (unadjusted)
Pixel computation	6.6 (5.92)	56.0 (50.3)
New Method	6.4 (5.77)	53.8 (50.2)

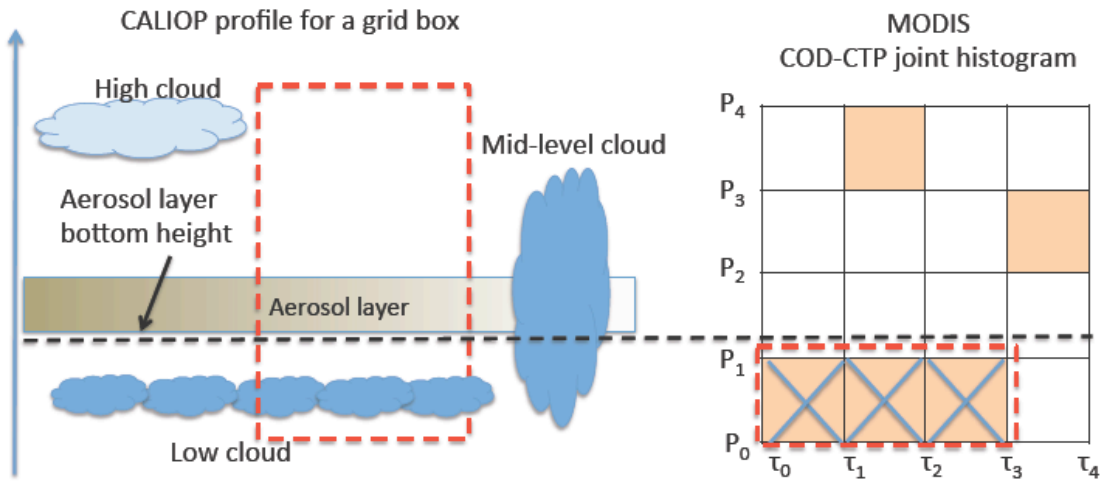

Figure 1 A schematic example to illustrate how CALIOP aerosol layer height information is used in our method to determine the population of liquid-phase clouds below the aerosol layer in the MODIS COD-CTP joint histogram.

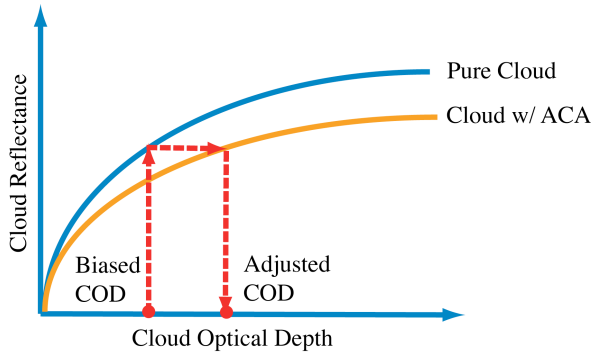

Figure 2 A schematic illustration of our fast scheme to correct the COD retrieval bias in the MODIS cloud product due to overlying aerosol contamination.

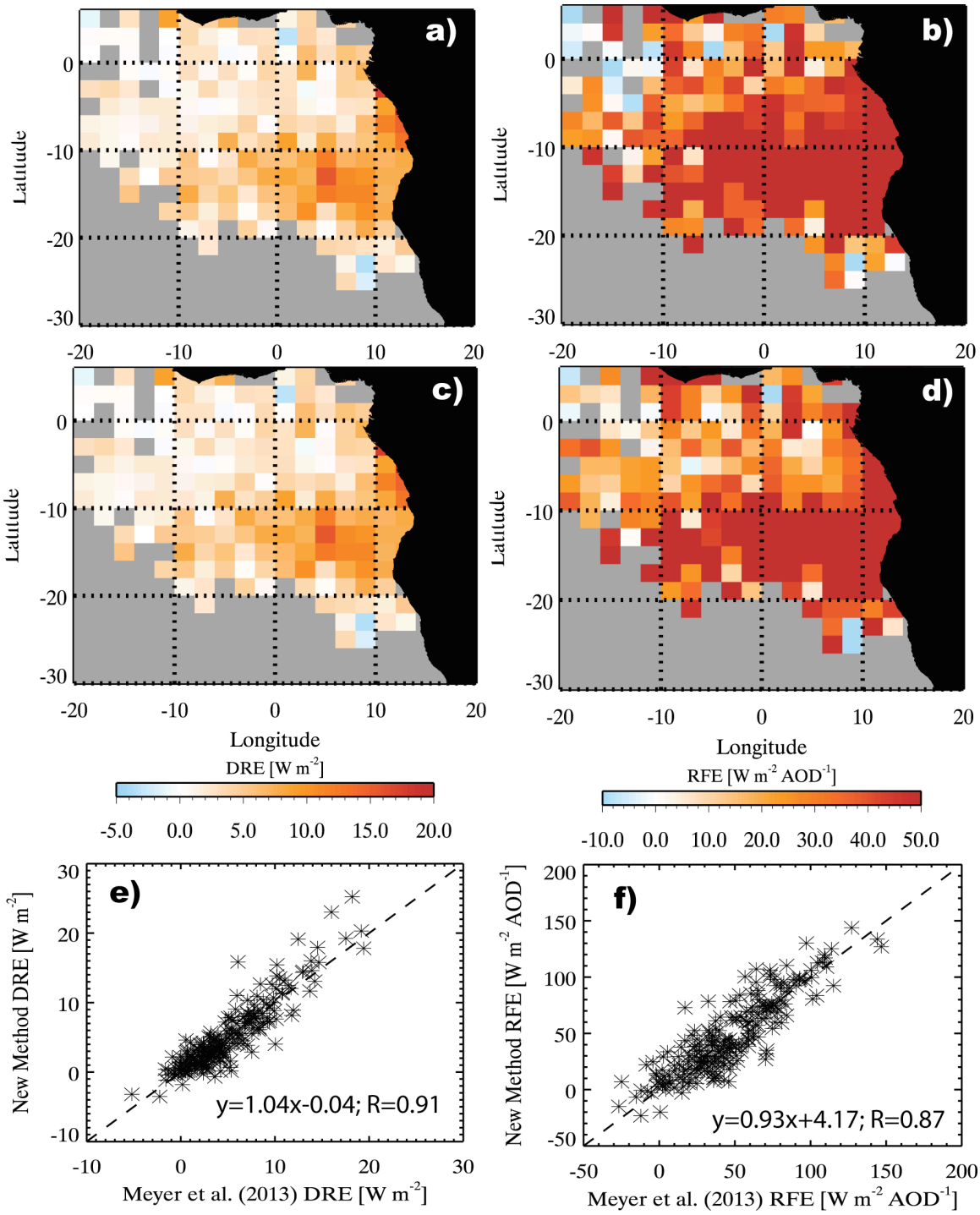

Figure 3 a) Seasonal mean (August/September 2007-2011) instantaneous TOA DRE of above-cloud smoke and polluted dust based on the pixel-level computations from (Meyer et al., 2013); b) seasonal mean instantaneous TOA aerosol RFE (i.e., DRE per AOD) from(Meyer et al., 2013); c) same as a), but based on the new method; d) same as b), but based on the new method.

1

2

3

4

5

6

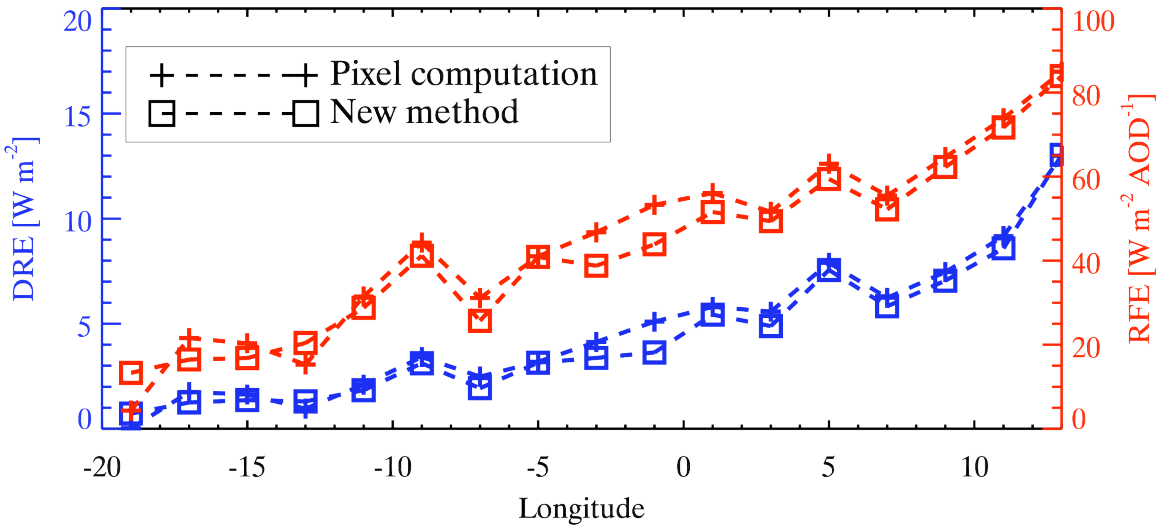

Figure 4 Meridional mean DRE and RFE for the region based on the results in Figure 3. Lines with cross symbol correspond to pixel computations from(Meyer et al., 2013). Lines with square symbol correspond to results based on the new method.

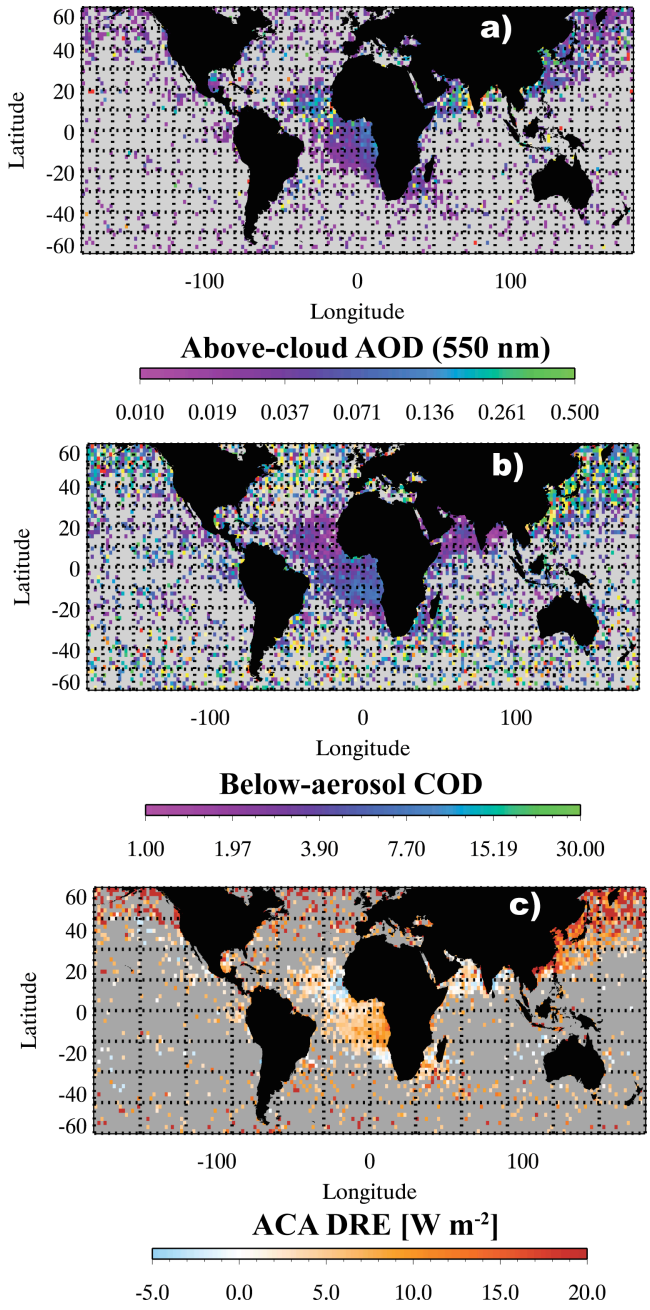

1

2 Figure 5 a) Annual mean AOD (at 550 nm) of above-cloud light-absorbing aerosols (i.e.,
3 smoke and polluted dust) derived from 4 years (2007~2010) of the CALIOP 5km aerosol
4 and cloud layer products. b) Annual mean below-aerosol COD derived from the MODIS
5 daily level-3 COD-CTP joint histogram. c) Annual mean instantaneous TOA DRE of
6 above-cloud light-absorbing aerosols derived using the new method.

7

Reference:

Abel, S. J., Highwood, E. J., Haywood, J. M. and Stringer, M. A.: The direct radiative effect of biomass burning aerosols over southern Africa, Atmospheric Chemistry and Physics, 5(7), 1999–2018, doi:10.5194/acp-5-1999-2005, 2005.

Ackerman, S., Strabala, K., Menzel, W., Frey, R., Moeller, C. and Gumley, L.: Discriminating clear sky from clouds with MODIS, Journal of Geophysical Research, 103(D24), 32,141–32,157, 1998.

Bergman, J. W. and Salby, M. L.: Diurnal Variations of Cloud Cover and Their Relationship to Climatological Conditions, Journal of Climate, 9(11), 2802–2820, doi:10.1175/1520-0442(1996)009<2802:DVOCCA>2.0.CO;2, 1996.

Chand, D., Anderson, T. L., Wood, R., Charlson, R. J., Hu, Y., Liu, Z. and Vaughan, M.: Quantifying above-cloud aerosol using spaceborne lidar for improved understanding of cloudy-sky direct climate forcing, J Geophys Res, 113(D13), doi:10.1029/2007JD009433, 2008.

Chand, D., Wood, R., Anderson, T. L., Satheesh, S. K. and Charlson, R. J.: Satellite-derived direct radiative effect of aerosols dependent on cloud cover, Nature Geoscience, 2(3), 181–184, doi:10.1038/ngeo437, 2009.

Clough, S. A., Shephard, M. W., Mlawer, E. J., Delamere, J. S., Iacono, M. J., Cady-Pereira, K., Boukabara, S. and Brown, P. D.: Atmospheric radiative transfer modeling: a summary of the AER codes, Journal of Quantitative Spectroscopy and Radiative Transfer VL -, 91(2), 233–244, 2005.

Coddington, O. M., Pilewskie, P., Redemann, J., Platnick, S., Russell, P. B., Schmidt, K. S., Gore, W. J., Livingston, J., Wind, G. and Vukicevic, T.: Examining the impact of overlying aerosols on the retrieval of cloud optical properties from passive remote sensing, J Geophys Res, 115(D10), doi:10.1029/2009JD012829, 2010.

Costantino, L. and Bréon, F. M.: Aerosol indirect effect on warm clouds over South-East Atlantic, from co-located MODIS and CALIPSO observations, Atmospheric Chemistry and Physics, 13(1), 69–88, doi:10.5194/acp-13-69-2013, 2013a.

Costantino, L. and Bréon, F. M.: Satellite-based estimate of aerosol direct radiative effect over the South-East Atlantic, Atmospheric Chemistry and Physics Discussions, 13(9), 23295–23324, doi:10.5194/acpd-13-23295-2013, 2013b.

de Graaf, M., Tilstra, L. G., Wang, P. and Stammes, P.: Retrieval of the aerosol direct radiative effect over clouds from spaceborne spectrometry, J Geophys Res, 117(D7), doi:10.1029/2011JD017160, 2012.

Devasthale, A. and Thomas, M. A.: A global survey of aerosol-liquid water cloud overlap

based on four years of CALIPSO-CALIOP data, Atmospheric Chemistry and Physics, 11(3), 1143–1154, doi:10.5194/acp-11-1143-2011, 2011.

Eck, T. F., Holben, B. N., Ward, D. E., Mukelabai, M. M., Dubovik, O., Smirnov, A., Schafer, J. S., Hsu, N. C., Piketh, S. J., Queface, A., Roux, J. L., Swap, R. J. and Slutsker, I.: Variability of biomass burning aerosol optical characteristics in southern Africa during the SAFARI 2000 dry season campaign and a comparison of single scattering albedo estimates from radiometric measurements, J. Geophys. Res., 108(D13), 8477, doi:10.1029/2002JD002321, 2003.

Hartmann, D., Holton, J. and Fu, Q.: The heat balance of the tropical tropopause, cirrus, and stratospheric dehydration, Geophys Res Lett, 28(10), 1969–1972, 2001.

Haywood, J. M., Osborne, S. R. and Abel, S. J.: The effect of overlying absorbing aerosol layers on remote sensing retrievals of cloud effective radius and cloud optical depth, Quarterly Journal of the Royal Meteorological Society, 130(598), 779–800, doi:10.1256/qj.03.100, 2004.

Hu, Y., Vaughan, M., Liu, Z., Lin, B., Yang, P., Flittner, D., Hunt, B., Kuehn, R., Huang, J., Wu, D., Rodier, S., Powell, K., Trepte, C. and Winker, D.: The depolarization - attenuated backscatter relation: CALIPSO lidar measurements vs. theory, Opt. Express, 15(9), 5327, doi:10.1364/OE.15.005327, 2007a.

Hu, Y., Vaughan, M., Liu, Z., Powell, K. and Rodier, S.: Retrieving Optical Depths and Lidar Ratios for Transparent Layers Above Opaque Water Clouds From CALIPSO Lidar Measurements, Geoscience and Remote Sensing Letters, IEEE DOI - 10.1109/LGRS.2007.901085, 4(4), 523–526, 2007b.

Hubanks, P. A., King, M. D., Platnick, S. and Pincus, R.: MODIS atmosphere L3 gridded product algorithm theoretical basis document, Algorithm Theor. Basis Doc. ATBD-MOD, 30, 2008.

Iacono, M. J., Delamere, J. S., Mlawer, E. J., Shephard, M. W., Clough, S. A. and Collins, W. D.: Radiative forcing by long-lived greenhouse gases: Calculations with the AER radiative transfer models, J. Geophys. Res., 113(D13), D13103, doi:10.1029/2008JD009944, 2008.

Ichoku, C., Remer, L. A., Kaufman, Y. J., Levy, R., Chu, D. A., Tanré, D. and Holben, B. N.: MODIS observation of aerosols and estimation of aerosol radiative forcing over southern Africa during SAFARI 2000, J. Geophys. Res., 108(D13), 8499, doi:10.1029/2002JD002366, 2003.

Jethva, H., Torres, O., Remer, L. A. and Bhartia, P. K.: A color ratio method for simultaneous retrieval of aerosol and cloud optical thickness of above-cloud absorbing aerosols from passive sensors: Application to MODIS measurements, IEEE TRANSACTIONS ON GEOSCIENCE AND REMOTE SENSING, 51(7), 3862–3870, 2013.

Jethva, H., Torres, O., Waquet, F., Chand, D. and Hu, Y.: How do A-train sensors intercompare in the retrieval of above-cloud aerosol optical depth? A case study-based assessment, Geophysical Research Letters, n/a–n/a, doi:10.1002/2013GL058405, 2014.

Keil, A. and Haywood, J. M.: Solar radiative forcing by biomass burning aerosol particles during SAFARI 2000: A case study based on measured aerosol and cloud properties, J Geophys Res, 108(D13), 8467, doi:10.1029/2002JD002315, 2003.

King, M. D., Platnick, S., Menzel, W. P., Ackerman, S. A. and Hubanks, P. A.: Spatial and Temporal Distribution of Clouds Observed by MODIS Onboard the Terra and Aqua Satellites, IEEE TRANSACTIONS ON GEOSCIENCE AND REMOTE SENSING, 51(7), 3826–3852, doi:10.1109/TGRS.2012.2227333, 2013.

Kistler, R., Collins, W., Saha, S., White, G., Woollen, J., Kalnay, E., Chelliah, M., Ebisuzaki, W., Kanamitsu, M., Kousky, V., van den Dool, H., Jenne, R. and Fiorino, M.: The NCEP–NCAR 50–Year Reanalysis: Monthly Means CD–ROM and Documentation, Bulletin of the American Meteorological Society, 82(2), 247–267, doi:10.1175/1520-0477(2001)082<0247:TNNYRM>2.3.CO;2, 2001.

Levy, R. C., Remer, L. A., Tanre, D., Mattoo, S. and Kaufman, Y. J.: Algorithm for remote sensing of tropospheric aerosol over dark targets from MODIS: Collections 005 and 051: Revision 2, MODIS Algorithm Theoretical Basis Document for the MOD04_L2 Product, 2009.

Liu, Z., Vaughan, M., Winker, D., Kittaka, C., Getzewich, B., Kuehn, R., Omar, A., Powell, K., Trepte, C. and Hostetler, C.: The CALIPSOLidar Cloud and Aerosol Discrimination: Version 2 Algorithm and Initial Assessment of Performance, Journal of Atmospheric and Oceanic Technology, 26(7), 1198–1213, doi:10.1175/2009JTECHA1229.1, 2009.

Liu, Z., Winker, D. M., Omar, A. H., Vaughan, M., Kar, J., Trepte, C. R. and Hu, Y.: Evaluation of CALIOP 532-nm AOD over Clouds, AGU Fall Meeting 2013, 2013.

Menzel, P., Frey, R., Baum, B. and Zhang, H.: Cloud Top Properties and Cloud Phase Algorithm Theoretical Basis Document. 2006.

Menzel, W., Smith, W. and Stewart, T.: Improved Cloud Motion Wind Vector and Altitude Assignment Using VAS, Journal of Applied Meteorology, 22(3), 377–384, 1983.

Meyer, K., Platnick, S., Oreopoulos, L. and Lee, D.: Estimating the direct radiative effect of absorbing aerosols overlying marine boundary layer clouds in the southeast Atlantic using MODIS and CALIOP, Journal of Geophysical Research-Atmospheres, n/a–n/a, doi:10.1002/jgrd.50449, 2013.

Min, M. and Zhang, Z.: **On the influence of cloud fraction diurnal cycle and sub-grid cloud optical thickness variability on all-sky direct aerosol radiative forcing**

, Journal of Quantitative Spectroscopy and Radiative Transfer, ((submitted)), n.d.

Myhre, G., Berntsen, T. K., Haywood, J. M., Sundet, J. K., Holben, B. N., Johnsrud, M. and Stordal, F.: Modeling the solar radiative impact of aerosols from biomass burning during the Southern African Regional Science Initiative (SAFARI-2000) experiment, J. Geophys. Res., 108(D13), 8501, doi:10.1029/2002JD002313, 2003.

Nakajima, T. and King, M.: Determination of the optical thickness and effective particle radius of clouds …, J Atmosph Sci, 1990.

Oikawa, E., Nakajima, T., Inoue, T. and Winker, D.: A study of the shortwave direct aerosol forcing using ESSP/CALIPSO observation and GCM simulation, J Geophys Res, 118, 3687–3708, doi:10.1002/jgrd.50227, 2013.

Omar, A. H., Winker, D. M., Vaughan, M. A., Hu, Y., Trepte, C. R., Ferrare, R. A., Lee, K.-P., Hostetler, C. A., Kittaka, C. and Rogers, R. R.: The CALIPSO automated aerosol classification and lidar ratio selection algorithm, Journal of Atmospheric and Oceanic Technology, 26(10), 1994–2014, 2009.

Oreopoulos, L., Cahalan, R. F. and Platnick, S.: The Plane-Parallel Albedo Bias of Liquid Clouds from MODIS Observations, Journal of Climate, 20(20), 5114–5125, doi:10.1175/JCLI4305.1, 2007.

Platnick, S., King, M., Ackerman, S., Menzel, W., Baum, B., Riedi, J. and Frey, R.: The MODIS cloud products: algorithms and examples from Terra, Geoscience and Remote Sensing, IEEE Transactions on, 41(2), 459–473, 2003.

Rossow, W. B. and Schiffer, R. A.: Advances in Understanding Clouds from ISCCP, Bulletin of the American Meteorological Society, 80(11), 2261–2287, doi:10.1175/1520-0477(1999)080<2261:AIUCFI>2.0.CO;2, 1999.

Rozendaal, M. A., Leovy, C. B. and Klein, S. A.: An Observational Study of Diurnal Variations of Marine Stratiform Cloud, Journal of Climate, 8, 1795–1809, 1995.

Schulz, J., Albert, P., Behr, H. D., Caprion, D., Deneke, H., Dewitte, S., Dürr, B., Fuchs, P., Gratzki, A., Hechler, P., Hollmann, R., Johnston, S., Karlsson, K. G., Manninen, T., Müller, R., Reuter, M., Riihelä, A., Roebeling, R., Selbach, N., Tetzlaff, A., Thomas, W., Werscheck, M., Wolters, E. and Zelenka, A.: Operational climate monitoring from space: the EUMETSAT Satellite Application Facility on Climate Monitoring (CM-SAF), Atmospheric Chemistry and Physics, 9(5), 1687–1709, doi:10.5194/acp-9-1687-2009, 2009.

Schulz, M., Textor, C., Kinne, S., Balkanski, Y., Bauer, S., Berntsen, T., Berglen, T., Boucher, O., Dentener, F., Guibert, S., Isaksen, I. S. A., Iversen, T., Koch, D., Kirkevåg, A., Liu, X., Montanaro, V., Myhre, G., Penner, J. E., Pitari, G., Reddy, S., Seland, Ø., Stier, P. and Takemura, T.: Radiative forcing by aerosols as derived from the AeroCom present-day and pre-industrial simulations, Atmos. Chem. Phys, 6, 5225–5246, 2006.

Stier, P., Schutgens, N. A. J., Bellouin, N., Bian, H., Boucher, O., Chin, M., Ghan, S., Huneeus, N., Kinne, S., Lin, G., Ma, X., Myhre, G., Penner, J. E., Randles, C. A., Samset, B., Schulz, M., Takemura, T., Yu, F., Yu, H. and Zhou, C.: Host model uncertainties in aerosol radiative forcing estimates: results from the AeroCom Prescribed intercomparison study, Atmospheric Chemistry and Physics, 13(6), 3245–3270, doi:10.5194/acp-13-3245-2013, 2013.

Torres, O., Jethva, H. and Bhartia, P. K.: Retrieval of Aerosol Optical Depth above Clouds from OMI Observations: Sensitivity Analysis and Case Studies, http://dx.doi.org/10.1175/JAS-D-11-0130.1, 69(3), 1037–1053, doi:10.1175/JAS-D-11-0130.1, 2012.

Twomey, S.: Atmospheric aerosols, Elsevier Scientific Publishing Co.,New York, NY. 1977.

Vaughan, M. A., Powell, K. A., Winker, D. M., Hostetler, C. A., Kuehn, R. E., Hunt, W. H., Getzewich, B. J., Young, S. A., Liu, Z. and McGill, M. J.: Fully Automated Detection of Cloud and Aerosol Layers in the CALIPSO Lidar Measurements, J. Atmos. Oceanic Technol., 26(10), 2034–2050, doi:doi: 10.1175/2009JTECHA1228.1, 2009.

Waquet, F., Cornet, C., Deuzé, J. L., Dubovik, O., Ducos, F., Goloub, P., Herman, M., Lapyonok, T., Labonnote, L. C., Riedi, J., Tanre, D., Thieuleux, F. and Vanbauce, C.: Retrieval of aerosol microphysical and optical properties above liquid clouds from POLDER/PARASOL polarization measurements, Atmos. Meas. Tech., 6(4), 991–1016, doi:10.5194/amt-6-991-2013, 2013a.

Waquet, F., Peers, F., Ducos, F., Goloub, P., Platnick, S., Riedi, J., Tanré, D. and Thieuleux, F.: Global analysis of aerosol properties above clouds, Geophysical Research Letters, n/a–n/a, doi:10.1002/2013GL057482, 2013b.

Waquet, F., Riedi, J., Labonnote, L. C., Goloub, P., Cairns, B., Deuzé, J. L. and Tanre, D.: Aerosol Remote Sensing over Clouds Using A-Train Observations, J Atmosph Sci, 66(8), 2468–2480, doi:10.1175/2009JAS3026.1, 2009.

Wilcox, E. M.: Stratocumulus cloud thickening beneath layers of absorbing smoke aerosol, Atmospheric Chemistry and Physics, 10(23), 11769–11777, doi:10.5194/acp-10-11769-2010, 2010.

Wilcox, E. M.: Direct and semi-direct radiative forcing of smoke aerosols over clouds, Atmospheric Chemistry and Physics, 12(1), 139–149, doi:10.5194/acp-12-139-2012, 2012.

Winker, D. M., Tackett, J. L., Getzewich, B. J., Liu, Z., Vaughan, M. A. and Rogers, R. R.: The global 3-D distribution of tropospheric aerosols as characterized by CALIOP, Atmospheric Chemistry and Physics, 13(6), 3345–3361, doi:10.5194/acp-13-3345-2013, 2013.

Winker, D. M., Vaughan, M. A., Omar, A., Hu, Y., Powell, K. A., Liu, Z., Hunt, W. H.

and Young, S. A.: Overview of the CALIPSO mission and CALIOP data processing algorithms, Journal of Atmospheric and Oceanic Technology, 26(11), 2310–2323, 2009.

Wiscombe, W. J.: Improved Mie scattering algorithms, Applied Optics, 19(9), 1505–1509, 1980.

Wood, R., Bretherton, C. S. and Hartmann, D. L.: Diurnal cycle of liquid water path over the subtropical and tropical oceans, Geophysical Research Letters, 29(23), 2092–, doi:10.1029/2002GL015371, 2002.

Young, S. A. and Vaughan, M. A.: The Retrieval of Profiles of Particulate Extinction from Cloud-Aerosol Lidar Infrared Pathfinder Satellite Observations (CALIPSO) Data: Algorithm Description, J. Atmos. Oceanic Technol., 26(6), 1105–1119, doi:doi: 10.1175/2008JTECHA1221.1, 2008.

Yu, H. and Zhang, Z.: New Directions: Emerging satellite observations of above-cloud aerosols and direct radiative forcing, Atmospheric Environment, 72(0), 36–40, doi:10.1016/j.atmosenv.2013.02.017, 2013.

Yu, H., Kaufman, Y. J., Chin, M., Feingold, G., Remer, L. A., Anderson, T. L., Balkanski, Y., Bellouin, N., Boucher, O. and Christopher, S.: A review of measurement-based assessments of the aerosol direct radiative effect and forcing, Atmospheric Chemistry and Physics, 6(3), 613–666, 2006.

Zelinka, M. D., Klein, S. A. and Hartmann, D. L.: Computing and partitioning cloud feedbacks using cloud property histograms. Part I: Cloud radiative kernels, Journal of Climate, 25(11), 3715–3735, doi:10.1175/JCLI-D-11-00248.1, 2012.

A novel method for estimating shortwave direct radiative effect of above-cloud aerosols using CALIOP and MODIS data

Zhibo Zhang[*,1,2], Kerry Meyer[3,4], Steven Platnick[4], Lazaros Oreopoulos[4], Dongmin Lee[4,5] and Hongbin Yu[4,6]

1. Department of Physics, University of Maryland, Baltimore County (UMBC), Baltimore, MD, USA
2. Joint Center Earth Systems & Technology (JCET), UMBC, Baltimore, MD, USA
3. Goddard Earth Sciences Technology and Research (GESTAR), Universities Space Research Association, Columbia, MD, USA
4. NASA Goddard Space Flight Center, Greenbelt, Maryland, USA
5. Goddard Earth Sciences Technology and Research (GESTAR), Morgan State University, Baltimore, MD, USA
6. Earth System Science Interdisciplinary Center, University of Maryland, College Park, MD, USA

- Corresponding author at: Department of Physics, UMBC, Baltimore, MD, 21250, USA, Tel: 410-455-6315,

  Email: Zhibo.Zhang@umbc.edu (Z. Zhang)

Revised for ***AMT***

Unknown
Field Code Changed

Unknown
Field Code Changed

Unknown
Field Code Changed

Zhibo Zhang 3/7/14 9:03 AM
Deleted: *To be submitted to*

Abstract

This paper describes an efficient and unique method for computing the shortwave direct radiative effect (DRE) of aerosol residing above low-level liquid-phase clouds using CALIOP and MODIS data. It addresses the overlap of aerosol and cloud rigorously by utilizing the joint histogram of cloud optical depth and cloud top pressure, while also accounting for sub-grid-scale variations of aerosols. The method is computationally efficient because of its use of grid-level cloud and aerosol statistics, instead of pixel-level products, and a pre-computed look-up table based on radiative transfer calculations. We verify that for smoke and polluted dust over the southeast Atlantic Ocean the method yields a seasonal mean *instantaneous* (approximately 1:30PM local time) shortwave DRE of above cloud aerosol (ACA) that generally agrees with more rigorous pixel-level computation within 4%. We also estimate the impact of potential CALIOP aerosol optical depth (AOD) retrieval bias of ACA on DRE. We find that the regional and seasonal mean *instantaneous* DRE of ACA over southeast Atlantic Ocean would increase, from the original value of 6.4 W m^{-2} based on operational CALIOP AOD to 9.6 W m^{-2} if CALIOP AOD retrievals are biased low by a factor of 1.5 (Meyer et al., 2013) and further to 30.9 W m^{-2} if CALIOP AOD retrievals are biased low by a factor of 5 as suggested in (Jethva et al., 2014). In contrast, the instantaneous ACA radiative forcing efficiency (RFE) remains relatively invariant in all cases at about 53 W m^{-2} AOD^{-1}, suggesting a near linear relation between the instantaneous RFE and AOD. We also compute the annual mean instantaneous shortwave DRE of light-absorbing aerosols (i.e., smoke and polluted dust) over global oceans based on 4 years of CALIOP and MODIS data. We find that given an above-cloud aerosol type the optical depth of the underlying clouds plays a larger role than above-cloud AOD in the variability of the annual mean shortwave DRE

Zhibo Zhang 3/7/14 9:03 AM
Deleted: accounts for

Zhibo Zhang 3/7/14 9:03 AM
Deleted: overlapping

Zhibo Zhang 3/7/14 9:03 AM
Deleted: . Effects of

Zhibo Zhang 3/7/14 9:03 AM
Deleted:

Zhibo Zhang 3/7/14 9:03 AM
Deleted: cloud and aerosol

Zhibo Zhang 3/7/14 9:03 AM
Deleted: on DRE are accounted for. It

Zhibo Zhang 3/7/14 9:03 AM
Deleted: through using

Zhibo Zhang 3/7/14 9:03 AM
Deleted: in radiative transfer calculations. We verified that for smoke over the southeast Atlantic Ocean the method yields a seasonal mean instantaneous shortwave DRE that generally agrees with more rigorous pixel-level computation within 4%. We have also computed

Zhibo Zhang 3/7/14 9:03 AM
Deleted: ocean

Zhibo Zhang 3/7/14 9:03 AM
Deleted: We found that

of above-cloud light-absorbing aerosol. While we demonstrate our method using CALIOP and MODIS data, it can also be extended to other satellite data sets.

Zhibo Zhang 3/7/14 9:03 AM
Deleted: is mainly driven by the optical depth of the underlying clouds.

1. Introduction

The shortwave direct radiative effect (DRE) of aerosols at the top of the atmosphere (TOA) is strongly dependent on the reflectance of the underlying surface. Over dark surfaces (e.g. ocean, vegetated land), the scattering effect of aerosols is generally dominant, leading to negative DRE (i.e., cooling) at TOA (Yu et al., 2006). In contrast, when light-absorbing aerosols occur above clouds or other bright surfaces (such as snow, ice, desert), aerosol absorption is significantly amplified by cloud or surface reflection, offsetting or even exceeding the scattering effect of the aerosol, leading to a less negative or even positive (i.e., warming) TOA DRE (Abel et al., 2005; Keil and Haywood, 2003; Twomey, 1977). Therefore, in order to understand the full complexity of aerosol radiative effects on climate, it is important to quantify the DRE under both clear-sky and cloudy-sky conditions. The DRE of aerosols in clear-sky regions has been extensively studied and is relatively well constrained based on advanced satellite remote sensing measurements acquired in the last decade (Yu et al., 2006). However, currently model simulations shows a large inter-model spread in cloudy-sky DRE (Schulz et al., 2006), which results from inter-model differences in both aerosol and cloud properties (Schulz et al., 2006; Stier et al., 2013). Therefore, there is a clear need for an observational constraint on the DRE of above-cloud aerosol (ACA).

Recent advances in satellite remote sensing techniques have provided an unprecedented opportunity for studying the DRE of ACA. In particular, the availability of measurements from the space-borne Cloud-Aerosol Lidar with Orthogonal Polarization (CALIOP) sensor onboard NASA's Cloud-Aerosol Lidar and Infrared Pathfinder

Zhibo Zhang 3/7/14 9:03 AM

Deleted: ocean, vegetated land), the scattering effect of aerosols is generally dominant, leading to negative DRE (i.e., cooling) at TOA (Yu et al., 2006). In contrast, when light-absorbing aerosols occur above clouds or other bright surfaces (such as snow, ice, desert), aerosol absorption is significantly amplified by cloud or surface reflection, offsetting or even exceeding the scattering effect of the aerosol leading to a less negative or even positive (i.e., warming) TOA DRE (Abel et al., 2005; Keil and Haywood, 2003; Twomey, 1977). Therefore, in order to understand the full complexity of aerosol radiative effects on climate, it is important to quantify the DRE under both clear-sky and cloudy-sky conditions. Although the DRE of aerosols in clear-sky regions has been extensively studied and is relatively well constrained based on advanced satellite remote sensing measurements acquired in the last decade (Yu et al., 2006), the cloudy-sky DRE is generally assumed to be negligible or simulated by models (Schulz et al., 2006). Currently model simulations shows a large inter-model spread in cloudy-sky DRE (Schulz et al., 2006), which results from inter-model differences in both aerosol and cloud properties (Schulz et al., 2006; Stier et al., 2013). There

Satellite Observations (CALIPSO) satellite has provided a revolutionary global view of the vertical distribution of aerosols and clouds (e.g., Winker et al., 2013). Using CALIOP aerosol and cloud layer products, Devasthale and Thomas (2011) found frequent occurrences of aerosols residing above low-level clouds in several regions of the globe. In particular, they found a high frequency of smoke occurrence over low clouds in the southeast Atlantic, western coasts of South America (e.g., Columbia, Ecuador, and Peru) and southern Asia. These authors also found a high frequency of natural and polluted dust aerosols overlapping low clouds off the western coasts of Saharan Africa in boreal summer and over boundary layer clouds in the eastern coast of China in boreal spring (see Fig. 3 of Devasthale and Thomas, 2011).

CALIOP measurements of ACA properties, in combination with satellite cloud products from, for example, the Moderate Resolution Imaging Spectroradiometer (MODIS), have been used in several recent studies to derive the DRE of ACA with radiative transfer simulations (e.g., Chand et al., 2009; Costantino and Bréon, 2013b; Meyer et al., 2013; Oikawa et al., 2013). (Chand et al., 2009) used CALIOP above-cloud AOD retrievals (Chand et al., 2008) and Terra-MODIS cloud products, both aggregated to 5º gridded monthly means, to calculate the radiative effects of smoke transported above the low-level stratocumulus deck in the southeastern Atlantic. The spatial-temporal aggregation of both CALIOP and MODIS data to coarse gridded monthly means obscures the potential influence of cloud and aerosol variability on the DRE. In particular, using grid box mean cloud optical depth for DRE calculation might lead to biases in DRE due to the plane-parallel albedo bias (Oreopoulos et al., 2007). Moreover, the MODIS level-3 aggregation algorithm samples all liquid water clouds, regardless of whether or

Zhibo Zhang 3/7/14 9:03 AM
Deleted: (e.g., Winker et al., 2013)

Zhibo Zhang 3/7/14 9:03 AM
Deleted: the eastern coast of China in boreal spring (see Fig. 3 of Devasthale and Thomas, 2011)

Zhibo Zhang 3/7/14 9:03 AM
Deleted: CALIOP measurements of ACA properties, in combination with satellite cloud products from, for example, the Moderate Resolution Imaging Spectroradiometer (MODIS), have been used in several recent studies to derive the DRE of ACA with radiative transfer simulations (e.g., Chand et al., 2009; Costantino and Bréon, 2013b; Oikawa et al., 2013). (Chand et al., 2009) used CALIOP above-cloud AOD retrievals (Chand et al., 2008) and Terra-MODIS cloud products, both aggregated to 5º gridded monthly means, to calculate the radiative effects of smoke transported above the low-level stratocumulus deck in the southeastern Atlantic. A major point made in this study is that the all-sky DRE of elevated light-absorbing aerosols, such as transported smoke, is strongly modulated by the underlying cloud properties. However, the spatial-temporal aggregation of both CALIOP and MODIS data to coarse gridded monthly means obscures the potential influence of cloud and aerosol variability on the DRE. In particular, using grid box mean cloud optical depth for DRE calculation might lead to biases in DRE due to the plane-parallel albedo bias (Oreopoulos et al., 2007). Moreover, the MODIS level-3 aggregation algorithm samples all liquid water clouds, regardless of possible retrieval contamination by ACA. As a result, the total population of liquid water clouds in the MODIS level-3 products (daily or monthly) may be significantly different from that of below-aerosol-only cloud population. Therefore, using level-3 MODIS products without distinguishing below-aerosol-only cloud population from the total can potentially lead to significant errors. The problem could be further complicated by biases in MODIS cloud retrievals associated with the presence of overlying light-absorbing aerosols. When a cloud-pixel is contaminated by overlying light-absorbing aerosols the MODIS cloud optical depth (COD) retrieval is generally biased low (Coddington et al., 2010; Haywood et al., 2004), an effect not considered in most previous studies (e.g., Chand et al., 2009; Costantino and Bréon, 2013b; Oikawa et al., 2013). Meyer et al. (2013) found that correcting the MODIS COD bias due to ACA contamination can lead to a more positive ACA DRE. ... [1]

not there is an aerosol layer above cloud. As a result, the total population of liquid water clouds in the MODIS level-3 products (daily or monthly) may be significantly different from that of below-aerosol-only cloud population. Therefore, using level-3 MODIS products without distinguishing below-aerosol-only from total cloud population can potentially lead to significant errors. The problem could be further complicated by biases in MODIS cloud retrievals associated with the presence of overlying light-absorbing aerosols. When a cloud-pixel is contaminated by overlying light-absorbing aerosols the MODIS cloud optical depth (COD) retrieval is generally biased low (e.g., Coddington et al., 2010; Haywood et al., 2004; Jethva et al., 2013; Wilcox, 2010), an effect not considered in most previous studies (e.g., Chand et al., 2009; Costantino and Bréon, 2013b; Oikawa et al., 2013). Most recently however, (Meyer et al., 2013) collocated CALIOP above-cloud AOD and Aqua-MODIS cloud properties at the pixel level, and the DRE was then computed at these individual collocated pixels. They found that correcting the MODIS COD bias due to ACA contamination leads to a more positive ACA DRE. Such rigorous collocation has obvious advantages as it takes into account the sub-grid variability of clouds and aerosols, but is on the other hand computationally expensive since it requires large amounts of pixel-level data that make global scale and multiyear studies challenging.

The objective of this paper is to describe a novel method for computing the DRE of ACA. This method attempts to balance the need for computational efficiency with the need for rigorous treatment of aerosol-cloud overlap and small-scale variability of aerosol and clouds. Our method has several unique features: 1) it takes sub-grid scale cloud and aerosol variation into account in DRE computations; 2) it treats the overlap of aerosol and

Zhibo Zhang 3/7/14 9:03 AM
Deleted: overlapping

Zhibo Zhang 3/7/14 9:03 AM
Deleted: variabilities

Zhibo Zhang 3/7/14 9:03 AM
Deleted: computation

Zhibo Zhang 3/7/14 9:03 AM
Deleted: overlapping

cloud rigorously by utilizing the joint histogram of COD and cloud top pressure (CTP) in the MODIS level-3 product; 3) it is computationally efficient because of the use of a pre-computed look-up table of ACA DRE.

In the following sections, we briefly introduce the CALIOP and MODIS data used (Section 2), describe the key assumptions and features of the novel method (Section 3), validate it through comparison with pixel-level computations as in (Meyer et al., 2013) (Section 4), and conclude with a summary and discussion (Section 5).

2. Satellite Data

In (Meyer et al., 2013), the MODIS level-2 cloud product is collocated with CALIOP level-2 aerosol product for every pixel along the CALIOP track and the computation of instantaneous DRE is performed pixel-by-pixel. Then, the pixel-level DRE results are aggregated on a latitude-longitude grid for climatological study. If only the grid-level DRE is of interest, the pixel-by-pixel computation of DRE may not be efficient because of redundant computations. For example, if two pixels with the same above-cloud AOD and below-cloud COD occur within the same grid-box, they evidently have the same ACA DRE, but the radiative transfer computation is nevertheless performed twice in the pixel-by-pixel method. As shown in Section 3, a more efficient way is to compute the DRE statistically using the probability density function (PDF) of above-cloud AOD and below-cloud COD. In this study, we use the CALIOP level-2 aerosol and cloud layer product (V3.01) to derive the statistics of ACA properties and the MODIS level-3 daily cloud product for cloud property statistics. It important to note that our method is not limited to CALIOP and MODIS products, but also applicable to other satellite data sets, such as above-cloud aerosol retrievals from POLDER (POLarization and Directionality

Zhibo Zhang 3/7/14 9:03 AM
Deleted: cloud optical depth

Zhibo Zhang 3/7/14 9:03 AM
Deleted:

Zhibo Zhang 3/7/14 9:03 AM
Deleted: assumption

Zhibo Zhang 3/7/14 9:03 AM
Deleted: (Meyer et al., 2013)

Zhibo Zhang 3/7/14 9:03 AM
Deleted: <#>CALIOP aerosol and cloud layer products ... [2]

of the Earth's Reflectances) (Waquet et al., 2009) and OMI (Ozone Monitoring Instrument)(Torres et al., 2012), and cloud retrievals from ISCCP (International Satellite Cloud Climatology Project) (Rossow and Schiffer, 1999) and SEVIRI (Spinning Enhanced Visible and Infrared Imager)(Schulz et al., 2009).

2.1. CALIOP level-2 aerosol and cloud layer products

Since its launch in 2006, the space-borne lidar CALIOP has continuously acquired, with near global (albeit instantaneously sparse) coverage, attenuated backscatter measurements at 532 nm and 1064 nm, including linear depolarization information at 532nm (Winker et al., 2009). The CALIOP level-2 retrieval algorithm consists of several steps. First, a "feature finder" algorithm and cloud-aerosol discrimination (CAD) algorithm are used to detect aerosol and cloud layers, and record their top and bottom heights and layer integrated properties (Vaughan et al., 2009). Second, the detected aerosol layers are further classified into six sub-types (i.e., polluted continental, biomass burning, desert dust, polluted dust, clean continental and marine) (Omar et al., 2009) and the detected cloud layers are assigned different thermodynamic phases (Hu et al., 2007a) based on the observed backscatter, color ratio and depolarization ratio. Third, *a priori* lidar ratios, pre-selected based on aerosol sub-type and cloud phase, are used to derive the extinction of an aerosol or cloud layer from the attenuated backscatter profile (Young and Vaughan, 2008).

In this study, we use CALIOP level-2 version 3.01 aerosol and cloud layer products at a nominal 5 km horizontal resolution (i.e., CAL_LID_L2_05kmALay and CAL_LID_L2_05kmCLay) for aerosol-cloud overlap detection, and for information on aerosol layer properties, including type, aerosol optical depth (AOD), and layer top and

Zhibo Zhang 3/7/14 9:03 AM
Deleted: overlapping

Zhibo Zhang 3/7/14 9:03 AM
Deleted: aerosol layer

bottom height. In addition to physical properties, the CALIOP layer products also provide various metrics and flags on data quality assurance. These include CAD score (Liu et al., 2009), horizontal averaging scale, extinction quality control (QC) flag, and estimated uncertainty of layer AOD. In this study, we apply these metrics following best practices provided by the CALIPSO science team to screen for reliable retrievals (e.g., Winker et al., 2013) (see Table 1).

It should be noted here that the current version of CALIOP operational aerosol retrieval algorithm (V3.01) appears to significantly underestimate the AOD of above-cloud aerosol layer according to recent studies (Jethva et al., 2014; Liu et al., 2013; Waquet et al., 2013b). The main reason is that after strong attenuation by the upper part of an aerosol layer, the 532 nm attenuated backscatter of the lower part of aerosol layer is often too small. As a result, the current CALIOP feature detection algorithm often cannot resolve the full depth of the aerosol layer, leading to low biases in retrieved AOD (Jethva et al., 2014; Liu et al., 2013). At the moment, the CALIOP operational team is investigating the possibility of using the algorithm described in (Chand et al., 2008; Hu et al., 2007b) for ACA retrievals (Liu et al., 2013). This alternate method utilizes the reflected lidar signal from the bright cloud layer underneath to derive the two-way transmittance and thereby the AOD of the ACA layer. Because the backscatter of a cloud layer is usually very strong, the two-way transmittance method is less affected by the strong attenuation of the ACA layer and is therefore expected to alleviate the aforementioned problem. Lidar based AOD retrievals are also known to suffer from other issues, such as the background solar noise during daytime. These issues are beyond the scope of this study, but are nevertheless discussed in the uncertainty analysis of Section

Zhibo Zhang 3/7/14 9:03 AM
Deleted: for

Zhibo Zhang 3/7/14 9:03 AM
Deleted: (Liu et al., 2009)

Zhibo Zhang 3/7/14 9:03 AM
Deleted: the

Zhibo Zhang 3/7/14 9:03 AM
Deleted: for

Zhibo Zhang 3/7/14 9:03 AM
Deleted: use

Zhibo Zhang 3/7/14 9:03 AM
Deleted: the

Zhibo Zhang 3/7/14 9:03 AM
Deleted: practice advice of

Zhibo Zhang 3/7/14 9:03 AM
Deleted: (e.g., Winker et al., 2013)

3.4.

In addition to retrieval errors and uncertainties, another limitation of CALIOP data is the small sampling rate (i.e., only along track). In order to compute the DRE of ACA over a given latitude-longitude grid box, we assume that the aerosol property statistics retrieved by CALIOP along its narrow track represent the statistics over the whole grid box, i.e., that AOD PDFs are identical. This assumption constitutes an uncertainty in our DRE computation. Due to a lack of satellite-based wide-swath ACA datasets, however, it is difficult to determine the size of this uncertainty. Recently, several novel methods have been developed to retrieve ACA properties from passive sensor observations (Jethva et al., 2013; Torres et al., 2012; Waquet et al., 2009; 2013a), which will help improve our understanding of the sub-grid ACA variability when they become available to public.

Finally, we emphasize two more points. First, none of the aforementioned problems with CALIOP data, e.g., smoke AOD bias, retrieval uncertainties, and small sampling rate, are unique to our method. Any method that uses CALIOP data faces the same challenges. Second, our method is not limited only to CALIOP data. We choose to use CALIOP product in this study solely because it is the only publically available ACA product at the moment. Our method can also be applied to other ACA retrieval products, based on for example, POLDER (Waquet et al., 2009), MODIS (Jethva et al., 2013), OMI (Torres et al., 2012) observations when they become available to public. In fact, as discussed later, the advantage of our method in terms of computational efficiency is even greater when applied on retrievals from passive sensors.

2.2. MODIS daily level-3 cloud property product

This study computes the grid-level ACA DRE using the statistics of aerosol and cloud properties, instead of pixel-by-pixel computation as in (Meyer et al., 2013). We use the Collection 5 (C5) Aqua MODIS level-3 *Daily* gridded Atmosphere product MYD08_D3 for the statistics of cloud properties and other parameters, such as solar zenith angle, needed for ACA DRE computations.

The MODIS level-3 (i.e., grid-level) product contains statistics computed from a set of level-2 (i.e., pixel-level) MODIS granules. As summarized in (Platnick et al., 2003), the operational level-2 MODIS cloud product provides cloud masking (Ackerman et al., 1998), cloud top height retrieval based on CO_2 slicing or the infrared window method (Menzel et al., 1983), cloud top thermodynamic phase determination (Menzel et al., 2006), and cloud optical and microphysical property retrieval based on the bi-spectral solar reflectance method (Nakajima and King, 1990). In addition to these cloud parameters, the level-2 products also provide pixel-level runtime Quality Assessment (QA) information, which includes product quality as well as processing path information. All MODIS level-2 atmosphere products, including the cloud, aerosol and water vapor products, are aggregated to 1° spatial resolution on a daily (product name MYD08_D3 for Aqua MODIS), eight-day (MYD08_E3), and monthly (MYD08_E3) basis. Aggregations include a variety of scalar statistical information (mean, standard deviation, max/min occurrences) and histograms (marginal and joint). A particularly useful level-3 cloud product for this study is the daily joint histogram of COD vs. CTP, derived using daily counts of successful daytime level-2 pixel retrievals that fall into each joint COD-CTP bin. Eleven COD bins, ranging from 0 to 100, and 13 CTP bins, ranging from 200 to

Zhibo Zhang 3/7/14 9:03 AM

Deleted: We use the Collection 5 (C5) Aqua MODIS level-3 daily gridded Atmosphere product (i.e., MYD08_D3) for cloud properties and other parameters, such as solar zenith angle, needed for ACA DRE computations. The MODIS level-3 gridded products are aggregated at 1° resolution from the MODIS level-2 pixel-level retrievals (Hubanks et al., 2008; King et al., 2003). As summarized in(Platnick et al., 2003), the operational level-2 MODIS cloud product provides cloud masking (Ackerman et al., 1998), cloud top height retrieval based on CO_2 slicing or the infrared window method (Menzel et al., 1983), cloud top thermodynamic phase determination (Menzel et al., 2006), and cloud optical and microphysical property retrieval based on the bi-spectral solar reflectance method (Nakajima and King, 1990). In addition to these cloud parameters, the level-2 products also provide pixel-level runtime Quality Assessment (QA) information, which includes product quality as well as processing path information. ... [3]

1000 mb, comprise the histogram. As discussed below, the COD-CTP joint histogram allows for identification of the portion of the cloud population that lies beneath the aerosol layer found by CALIOP, as well as the corresponding COD probability distribution needed for DRE estimation. In addition to the COD-CTP joint histogram, we also use the gridded mean solar and sensor zenith angles for calculating DRE and correcting the COD bias due to the presence of ACA.

It should be noted that the level-3 daily product MYD08_D3 contains statistics computed from a set of level-2 MODIS granules that theoretically span a 24-hour interval (Hubanks et al., 2008). However, for cloud parameters retrieved only during daytime, such as COD and cloud droplet effective radius (CER), only daytime level-2 files are used to compute the level-3 daily statistics. These are called *daytime only* SDSs (Scientific Data Sets) in level-3 products. Strictly speaking, the *daytime only* SDSs of only those 1° gridcells between approximately 23° N and 23° S come from a single MODIS overpass. The tropical southeast Atlantic region, where transported smoke aerosols are often observed above low-level stratocumulus clouds, is well within this range (about 10° N~30° S see Figure 3). The COD statistics in MYD08_D3 product for this region are therefore derived from a single Aqua-MODIS overpass that can be collocated with CALIOP observations (see Section 3.1 for details on collocation). The DRE computed based on the collocated dataset is therefore *instantaneous* DRE at Aqua crossing time (1:30PM) that are directly comparable to the pixel-by-pixel results in (Meyer et al., 2013). Poleward of 23°, MYD08_D3 statistics are derived from averaging several overlapping orbits approximately 100 minutes apart (Hubanks et al., 2008). As a result, strictly speaking the DRE computed for mid and high latitude regions based on

MYD08_D3 data is not *instantaneous* DRE. We emphasize that this is not a limitation of our method, but an inherent characteristic of the MODIS level-3 product.

3. Methodology

3.1. Theoretical basis

As in previous investigations (e.g., Chand et al., 2008; 2009; Costantino and Bréon, 2013b; Meyer et al., 2013), we focus on the simplest case of overlapping aerosol and cloud, i.e., a single layer of aerosol overlying a single layer of low-level liquid-phase clouds, which is commonly observed in many regions of the globe (Devasthale and Thomas, 2011). More complex situations certainly exist, such as an aerosol layer located in between high and low cloud, or an aerosol layer overlying multiple layers of clouds. However, identification of such situations are either beyond the detection capabilities of CALIOP or relatively rare (Devasthale and Thomas, 2011). As such, they are not considered here and left for future research.

To illustrate the theoretical foundation of the method, consider the schematic example in Figure 1. For a given grid box (e.g., 1°×1° in case of MODIS level-3 data), the gridded mean *instantaneous* broadband shortwave DRE ($\langle DRE \rangle_{ACA}$) averaged over all ACA pixels within the grid box is given by:

$$\langle DRE \rangle_{ACA} = \int_0^\infty \int_0^\infty DRE(\tau_c, \tau_a) p(\tau_c, \tau_a) d\tau_c d\tau_a, \quad (1)$$

where $p(\tau_c, \tau_a)$ is the joint probability density function (PDF) of the above-cloud AOD at 532 nm (τ_a) and below-aerosol COD (τ_c) of ACA pixels. We note that, in addition to τ_a, DRE also depends on the spectral variation of aerosol and cloud optical depth, spectral single scattering albedo and asymmetry factor, wavelength dependencies not

Zhibo Zhang 3/7/14 9:03 AM
Deleted: ,

Unknown
Field Code Changed

Zhibo Zhang 3/7/14 9:03 AM
Deleted: is

Zhibo Zhang 3/7/14 9:03 AM
Deleted: a function

Zhibo Zhang 3/7/14 9:03 AM
Deleted: wavelength dependence of AOD

Zhibo Zhang 3/7/14 9:03 AM
Deleted: which are

explicitly shown in this equation. These properties are computed using a Mie scattering code (Wiscombe, 1980) based on the aerosol model described in (Meyer et al., 2013). The dependencies on solar zenith angle, surface reflectance, cloud particle effective radius, and atmospheric profile are also omitted from the equation; solar zenith angle and surface reflectance are expected to have only minor variation within the grid box, while the impact of cloud particle effective radius and atmospheric profile on shortwave DRE is relatively small. Since $p(\tau_c,\tau_a)$ describes the covariation of aerosols and clouds for the ACA pixels, it should ideally be derived from collocated CALIOP aerosol and MODIS cloud retrievals at pixel level as in (Meyer et al., 2013). However, this requires large amounts of pixel-level data. Therefore, pixel-level collocation and radiative transfer simulation are too computationally expensive and cumbersome for multiyear global studies.

A key assumption in our method, which allows us to avoid tedious pixel-level collocation, is that the *sub-grid level instantaneous* spatial distribution of above-cloud AOD is statistically independent from the *sub-grid level instantaneous* spatial distribution of below-aerosol COD. Under this assumption, $p(\tau_c,\tau_a)=p(\tau_c)\cdot p(\tau_a)$ and Eq. (1) reduces to:

$$\langle DRE\rangle_{ACA}=\int_0^\infty\left[\int_0^\infty DRE(\tau_c,\tau_a)p(\tau_c)d\tau_c\right]p(\tau_a)d\tau_a, \quad (2)$$

where $p(\tau_c)$ and $p(\tau_a)$ are the PDF of *instantaneous* below-aerosol COD τ_c and above-cloud AOD τ_a, respectively, of ACA pixels. The advantage of Eq. (2) is that it allows $p(\tau_c)$ and $p(\tau_a)$ to be derived separately and independently. This assumption is

Zhibo Zhang 3/7/14 9:03 AM
Deleted: included

Zhibo Zhang 3/7/14 9:03 AM
Deleted: (Wiscombe, 1980)

Zhibo Zhang 3/7/14 9:03 AM
Deleted: (Meyer et al., 2013).

Zhibo Zhang 3/7/14 9:03 AM
Deleted: (Meyer et al., 2013). This requires large amounts of pixel-level data, however, as one month of global daytime C5 MODIS level-2 cloud products in HDF format are roughly 150 Gigabytes.

Zhibo Zhang 3/7/14 9:03 AM
Deleted: and below-aerosol COD are

Zhibo Zhang 3/7/14 9:03 AM
Deleted: $\langle DRE\rangle_{ACA}=\int_0^\infty\left[\int_0^\infty DRE(\tau_c$

Unknown
Field Code Changed

reasonable considering that transported ACAs and low-level boundary layer clouds are usually well separated vertically (Devasthale and Thomas, 2011) and controlled by different meteorological conditions. The potential coupling between the two is that overlying absorbing aerosols could influence the evolution of clouds through changing atmospheric stratification (Wilcox, 2010). However, a recent observational study (Costantino and Bréon, 2013a) found no correlation between above-cloud AOD and below-aerosol COD, although correlations are found between AOD and cloud droplet effect radius, as well as liquid water path. Moreover, it is important to stress that our assumption is that the *instantaneous* above-cloud AOD and below-aerosol COD are independent *at sub-grid scale*. This assumption does not rule out the possibility that AOD and COD could be correlated at longer temporal (e.g., seasonal) and/or larger spatial (e.g., regional) scale through the thermodynamic and radiative coupling (Wilcox, 2010; 2012). Finally, as shown in section 4, when we compare the DRE derived from pixel-level collocation (i.e., based on Eq. (1)) with that from independent sampling of $p(\tau_c)$ and $p(\tau_a)$ (i.e., based on Eq. (2)) the agreement is very good.

In our method, the PDF of above-cloud AOD $p(\tau_a)$ is derived from the CALIOP 5km aerosol and cloud layer products through the following steps: 1) for each 5km CALIOP profile that falls within a given latitude-longitude grid box, we first search for an aerosol layer; 2) if an aerosol layer is detected and the quality metrics pass the quality assurance criteria summarized in Table 1, we then proceed to check for the presence of an underlying liquid-phase cloud layer within the profile using the CALIOP cloud layer product; 3) if a cloud layer is present, the AOD of the aerosol layer is recorded for the

Zhibo Zhang 3/7/14 9:03 AM
Deleted: (Devasthale and Thomas, 2011)

Zhibo Zhang 3/7/14 9:03 AM
Deleted: (Costantino and Bréon, 2013a)

Zhibo Zhang 3/7/14 9:03 AM
Deleted: . Moreover, as shown in section 4, we have compared

Zhibo Zhang 3/7/14 9:03 AM
Deleted: $p(\tau_c)$ and $p(\tau_a)$ (

Zhibo Zhang 3/7/14 9:03 AM
Deleted: and found

Zhibo Zhang 3/7/14 9:03 AM
Deleted: agreement.

derivation of the $p(\tau_a)$ of the grid box. The bottom height of the aerosol layer is also recorded to derive the grid mean aerosol layer bottom height. Once all of the CALIOP profiles within the grid box are processed, we obtain the PDF of the above-cloud AOD $p(\tau_a)$ and the mean aerosol layer bottom pressure $\langle P_{bottom} \rangle$.

As schematically illustrated in Figure 1, the PDF of below-aerosol COD $p(\tau_c)$ is derived from the joint histogram of cloud optical depth and cloud top pressure (COD-CTP joint histogram) in the MODIS daily level-3 product, using the grid mean aerosol layer bottom pressure $\langle P_{bottom} \rangle$ derived above. For a given grid box, we first identify the population of liquid-phase clouds below the pressure level $\langle P_{bottom} \rangle$. This subset, together with the AOD PDF $p(\tau_a)$, is then used to calculate DRE according to Eq. (2).

Zhibo Zhang 3/7/14 9:03 AM
Deleted: $\langle p_{bottom} \rangle$

In this study, we focus on the computation of instantaneous DRE. To obtain diurnally averaged DRE, technically speaking one would simply need to integrate over time the instantaneous DRE. However, it is important to note that, in addition to diurnal variation of solar zenith angle, aerosol and cloud properties may also have significant diurnal cycles. In fact, it is known that the low cloud fraction over stratocumulus regimes, such as the South East Atlantic region, have a strong diurnal cycle (15~35% of diurnal mean value) driven by cloud solar absorption(Wood et al., 2002). A recent study by (Min and Zhang, n.d.) indicates that using a constant cloud fraction based on Aqua-MODIS observations tends to result in significantly underestimated diurnal mean DRE even if the diurnal variation of solar zenith angle is considered in the computation. Therefore, the diurnal variation of cloud properties is an important factor to consider in the inter-

comparison of DRE computations based on different datasets and inter-comparison between observational study and modeling results.

3.2. DRE Look-up Tables

To speed up calculations, we use pre-computed aerosol-type specific look-up-tables (LUTs), instead of online radiative transfer computation, when deriving the DRE of ACA. The concept of our LUTs is somewhat similar to the "radiative kernels" described in (Hartmann et al., 2001) and (Zelinka et al., 2012) for computing cloud radiative feedbacks. The LUT for each aerosol type consists of DREs at both TOA and surface (not used in this study) for various combinations of AOD, COD, CTP and solar zenith conditions. As such, once the aerosol type and AOD are known from CALIOP and COD, CTP and solar zenith angle are known from MODIS, the corresponding DRE can be obtained through LUT interpolation. Note that the CALIOP only provides AOD at lidar wavelengths (e.g., 532 nm and 1064 nm) for each aerosol type. Therefore, radiative transfer model-appropriate narrowband aerosol scattering properties, namely AOD, single-scattering albedo and asymmetry factor, are needed for the development of the LUT. The current version of LUT focuses on light-absorbing aerosols (e.g., smoke and polluted dust). In order to validate our method with more rigorous pixel-level computations, we adopt the narrowband aerosol optical properties of (Meyer et al., 2013), who used the same radiative transfer code, in the computation of the current LUT. The aerosol model in (Meyer et al., 2013) is extended from an absorbing aerosol model developed for the MODIS Collection 5 Aerosol Product (MOD04) (see Table 4 of Levy et al., 2009). The MOD04 aerosol models define aerosol size distributions and refractive indices based solely on prescribed AOD at 550 nm (MODIS band 4; note that the

Zhibo Zhang 3/7/14 9:03 AM

Deleted: For better computational efficiency, we use pre-computed aerosol-type specified look-up-tables (LUTs), instead of online radiative transfer computation, when deriving the DRE of ACA. The concept of our LUTs is somewhat similar to the "radiative kernels" described in (Hartmann et al., 2001) and (Zelinka et al., 2012) for computing cloud radiative feedbacks. The LUT for each aerosol type consists of DREs at both TOA and surface (not used in this study) for various combinations of AOD, COD, CTP and solar zenith conditions. As such, once the aerosol type and AOD are known from CALIOP and COD, CTP and solar zenith angle are known from MODIS, the corresponding DRE can be obtained through LUT interpolation. Note that the CALIOP only provides AOD at lidar wavelengths (e.g., 532 nm and 1064 nm) for each aerosol type. Therefore, broadband aerosol scattering properties, including spectrally dependent AOD, single-scattering albedo and asymmetry factor, are needed for the development of LUT. The current version of LUT focuses on light-absorbing aerosols (e.g., smoke and polluted dust). In order to validate our method with more rigorous pixel-level computations, we adopt the broadband aerosol optical properties from (Meyer et al., 2013) in the computation of the current LUT. The aerosol model in (Meyer et al., 2013) is extended from an absorbing aerosol model developed for the MODIS Collection 5 Aerosol Product (MOD04) (see Table 4 of Levy et al., 2009). The MOD04 aerosol models define aerosol size distributions and refractive indices dependent solely on prescribed AOD at 550 nm (MODIS band 4; note that the absorbing aerosol model used here assumes a constant index of refraction, 1.51–0.02i, at all wavelengths). At AOD=0.5 (550 nm), the single-scattering albedo of this model is about 0.9 over the visible spectral region (see Figure 7 of Meyer et al., 2013), which is in the range of previously reported values (e.g., Keil and Haywood, 2003; Myhre et al., 2003). The current AOD bins (at 550 nm) in the LUT range from 0.05 to 1.5, which covers most of the above-cloud AOD observed by CALIOP. The current COD bins, logarithmically spaced, range from 0.1 to 300. Following the MODIS level-3 data, the thirteen CTP bins range from 1000mb to 200mb. The solar zenith angle bins range from 0 to 80 degree. Radiative transfer computations are carried out using the RRTM-SW model (Clough et al., 2005; Iacono et al., 2008). Lambertian ocean surface reflectance is set to 5%. Cloud droplet effective radius is fixed at 15 μm, which is close to the global mean value over oceans observed by MODIS (King et al., 2013). Water cloud optical properties are calculated internally by R ... [4]

absorbing aerosol model used here assumes a constant index of refraction, 1.51–0.02i, at all wavelengths). At AOD=0.5 (550 nm), the single-scattering albedo of this model is about 0.9 over the visible spectral region (see Figure 7 of Meyer et al., 2013), which is in the range of previously reported values (e.g., Keil and Haywood, 2003; Myhre et al., 2003). The current AOD bins (at 550 nm) in the LUT range from 0.05 to 1.5, which covers most of the above-cloud AOD observed by CALIOP. The current COD bins, logarithmically spaced, range from 0.1 to 300. Following the MODIS level-3 data, the thirteen CTP bins range from 1000mb to 200mb. The solar zenith angle bins range from 0 to 80 degree. Radiative transfer computations are carried out using the RRTM-SW model (Clough et al., 2005; Iacono et al., 2008). Lambertian ocean surface reflectance is set to 5%. Cloud droplet effective radius is fixed at 15 μm, which is close to the global mean value over oceans observed by MODIS (King et al., 2013). This value of effective radius is also used to convert the MODIS visible COD to liquid water path used as input to RRTM-SW. Liquid cloud optical properties are calculated internally by RRTM. For atmospheric profiles of water vapor and temperature, we use NCEP R1 reanalysis data (Kistler et al., 2001) averaged both zonally and annually. Our sensitivity tests indicate that the shortwave DRE of ACA is largely insensitive to cloud effective radius or atmospheric profiles.

3.3. Cloud Optical Depth Correction

As noted in previous studies (Coddington et al., 2010; e.g., Haywood et al., 2004), when a cloudy MODIS pixel is contaminated by overlying light-absorbing aerosols the COD retrieval is generally biased low. We have developed a fast COD correction scheme to account for the COD retrieval bias due to ACA in our DRE computation, which is

Zhibo Zhang 3/7/14 9:03 AM
Deleted: (Coddington et al., 2010; e.g., Haywood et al., 2004)

illustrated in Figure 2. This scheme requires both the cloud reflectance LUT for clouds without ACA, for which we use the MODIS operational LUT, and clouds with ACA, for which we use the one developed by Meyer et al. (2013). In the operational MODIS retrieval, the reflectance LUT of cloud without ACA is used to interpret the reflectance of all clouds, including those affected by ACA. Based on this fact, we first infer the "observed" cloud reflectance (after atmospheric correction) by interpolating the reflectance LUT of cloud without ACA corresponding to the biased COD. Then, we use the "observed" cloud reflectance and ACA-affected LUT (derived based on CALIOP AOD) to determine the corrected COD. This COD correction process is performed for every combination of COD bin in $p(\tau_c)$ and AOD bin in $p(\tau_a)$. In the final step we resample the corrected CODs to obtain the corrected $p(\tau_c)$.

It should be noted that because different aerosol type may have different impact on MODIS COD retrievals, the above COD correction process is aerosol-type dependent. In this study, we use light-absorbing aerosols as example to illustrate our method and for validation purposes we use the aerosol model developed by (Meyer et al., 2013) for the development of LUTs for DRE computation and COD correction. However, the LUTs can be easily extended to other aerosol models. In fact, as part of ongoing research, we are extending our LUTs to include all six operational CALIOP aerosol models as described in (Omar et al., 2009).

Zhibo Zhang 3/7/14 9:03 AM
Deleted: purpose

Zhibo Zhang 3/7/14 9:03 AM
Deleted: in(Meyer et al., 2013)

Unknown
Field Code Changed

3.4. Uncertainty Analysis

Several recent studies suggest that the current operational CALIOP product tends to underestimate the above-cloud AOD. Meyer et al. (2013) found that the daytime CALIOP AOD retrievals are systematically smaller than the nighttime retrievals,

probably due to the daytime solar background issue. In the light of this finding, Meyer et al. (2013) increased the CALIOP AOD retrievals by a factor of 1.5 to account for the impact of potential AOD bias on DRE of ACA. A more recent case study by (Jethva et al., 2014) suggests that CALIOP ACA AOD retrievals are biased low by a factor of 5 or even more compared with other retrievals, although the generality of this finding needs to be further tested with larger samples. While a rigorous analysis uncertainty analysis of CALIOP AOD product is beyond the scope of this study, it is nevertheless reasonable to assume that the current CALIOP retrievals provide a lower limit to the ACA AOD. In the uncertainty analysis presented in the next section, we carry out two sensitivity tests to estimate the potential impacts of CALIOP AOD bias on DRE computation. We multiply CALIOP AOD values by a factor of 1.5 in the first test following (Meyer et al., 2013) and by a factor of 5 in the second as suggested in (Jethva et al., 2014).

Once the magnitude of the uncertainties in the input data is prescribed, the consequential impact on DRE can be easily estimated in our method as follows. First, in addition to the $p(\tau_a)$ based on the original CALIOP data, we also derive the perturbed PDF $\tilde{p}(\tau_a)$ by perturbing the original data according to pre-defined uncertainties (i.e., by increasing the original values by a factor of 1.5 or 5). Then, the impact of input uncertainty on ACA DRE can be estimated by comparing the DREs computed with the original vs. perturbed PDF (i.e., $\langle DRE \rangle_{ACA}$ vs. $\langle \widetilde{DRE} \rangle_{ACA}$). Note that $\langle DRE \rangle_{ACA}$ and $\langle \widetilde{DRE} \rangle_{ACA}$ can be obtained in a single computation because they both represent integrals over $DRE(\tau_c, \tau_a)$, only with different weights. In this regard, our method is much more

efficient than the pixel-by-pixel method, in which uncertainty must be estimated by perturbing individual pixels.

4. Implementation and validation of new DRE estimation scheme

Each year during austral winter, dry season biomass burning activities throughout southern Africa inject large amounts of smoke into the troposphere (Eck et al., 2003; Ichoku et al., 2003; Myhre et al., 2003). Prevailing easterly winds during this season often transport the smoke westward off the continent, over the ocean, where extensive marine boundary layer clouds persist for most of the year. Under the descending branch of the Hadley cell, the air mass above the boundary layer is quite dry. Due to the lack of efficient wet scavenging, the transported aerosol layers can remain suspended in the atmosphere for days, creating a near-persistent smoke layer above the stratocumulus deck over the southeastern Atlantic Ocean (Chand et al., 2009; Devasthale and Thomas, 2011; Keil and Haywood, 2003; Wilcox, 2010).

To validate our method, we have compared the DRE of above-cloud light-absorbing aerosols in this region with pixel-level computations from (Meyer et al., 2013). Figure 3a shows the seasonal mean (August/September 2007-2011) instantaneous TOA DRE of above-cloud smoke and polluted dust based on the pixel-level computations from (Meyer et al., 2013). Figure 3b shows the corresponding instantaneous TOA aerosol radiative forcing efficiency (RFE) defined as the DRE per unit AOD. The DRE and RFE results computed using our method described in the previous section are shown in Figure 3c and Figure 3d, respectively. Evidently, both DRE and RFE computed using our new method agree closely with the pixel-level computations. Figure 4 shows the meridional mean DRE and RFE for the region using the results in Figure 3. Not surprisingly, the outcomes

Zhibo Zhang 3/7/14 9:03 AM
Deleted: Each year during austral winter, dry season biomass burning activities throughout southern Africa inject large amounts of smoke into the troposphere (Eck et al., 2003; Ichoku et al., 2003; Myhre et al., 2003). Prevailing easterly winds during this season often transport the smoke westward off the continent, over the ocean, where extensive marine boundary layer clouds persist for most of the year. Under the descending branch of the Hadley cell, the air mass above the boundary layer is quite dry. Due to the lack of efficient wet scavenging, the transported aerosol layers can remain suspended in the atmosphere for days, creating a near-persistent smoke layer above the stratocumulus deck over the southeastern Atlantic Ocean during this time (Chand et al., 2009; Devasthale and Thomas, 2011; Keil and Haywood, 2003; Wilcox ... [5]

Zhibo Zhang 3/7/14 9:03 AM
Deleted: (Meyer et al., 2013)

Zhibo Zhang 3/7/14 9:03 AM
Deleted: based on

Zhibo Zhang 3/7/14 9:03 AM
Deleted: results based on

of the two methods are almost identical. Note that the CODs used in the computations for Figure 3 and Figure 4 are directly from the MODIS products without COD correction. We have also compared the DRE and RFE from the two methods using the corrected COD and achieved again very good agreement (not shown because of close resemblance to Figure 3 and Figure 4). The seasonal and regional mean DRE and RFE, based on the corrected COD, from the pixel-level computation method in (Meyer et al., 2013) are 6.6 W m^{-2} and 56 W m^{-2} AOD^{-1}, respectively (see Table 2). The corresponding values from our new method are 6.4 W m^{-2} and 53.8 W m^{-2} AOD^{-1}, respectively.

As previously mentioned, to estimate potential bias in CALIOP ACA AOD retrieval on our DRE computation, we carried out two sensitivity tests. We increased CALIOP AOD values by a factor of 1.5 in one test following (Meyer et al., 2013) (hereafter refered to as "x1.5 test") and by a factor of 5 in another as suggested in (Jethva et al., 2014) ("x5.0 test" hereafter). In both cases, we corrected the MODIS COD retrievals based on the scaled AOD. The regional and seasonal mean DRE of ACA increases, from the original value of 6.4 W m^{-2} to 9.6 W m^{-2} in the x1.5 test and to 30.9 W m^{-2} in the x5.0 test. We have to note that this is a very rough estimate. Nevertheless, the DRE based on the x1.5 scaling of CALIOP AOD seems to agree reasonably with the value, 9.2±6.6 W m^{-2}, reported in an independent study by Wilcox (Wilcox, 2012). Interestingly, the scaling of AOD has little impact on RFE in both cases (53.1 W m^{-2} AOD^{-1} in the x1.5 case and 51.2 W m^{-2} AOD^{-1} in the x5.0 case), which apparently suggests a near linear relationship between DRE and AOD as also noted in (Meyer et al., 2013) and (Wilcox, 2012) (see his Figure 5).

Zhibo Zhang 3/7/14 9:03 AM
Deleted: based on

Zhibo Zhang 3/7/14 9:03 AM
Deleted: these results are

Zhibo Zhang 3/7/14 9:03 AM
Deleted: here

Zhibo Zhang 3/7/14 9:03 AM
Deleted: they are quite similar

Zhibo Zhang 3/7/14 9:03 AM
Deleted: those in

Zhibo Zhang 3/7/14 9:03 AM
Deleted: (Meyer et al., 2013) are 6.63 W m^{-2} and 55.97

Zhibo Zhang 3/7/14 9:03 AM
Deleted: 39

Zhibo Zhang 3/7/14 9:03 AM
Deleted: 77

In summary, as shown clearly in Figure 3, Figure 4 and Table 2, the DRE inferred from our new method agrees very well with the pixel-level computations. Furthermore, the difference between the two methods is much smaller than, for example, the uncertainty associated with CALIOP retrieval biases.

It is worthwhile to clarify again that the results shown in Figure 3 are seasonal mean *instantaneous* DRE at A-Train crossing time (1:30PM local time) based on CALIOP above-cloud AOD and corrected Aqua MODIS below-aerosol COD retrievals. Moreover, the aerosol model described in (Meyer et al., 2013) is used in this study. All these factors should be considered when comparing the results in this study with those in other studies (e.g., Chand et al., 2009; de Graaf et al., 2012; Wilcox, 2012). For example, (Chand et al., 2009) used CALIOP in combination with Terra-MODIS observation to compute the DRE over the South East Atlantic Region. It is known that low-clouds in this region have a strong diurnal cycle driven by solar cloud absorption (Bergman and Salby, 1996; Rozendaal et al., 1995; Wood et al., 2002). As a result the cloud properties observed by Terra-MODIS can be significantly different from those observed by Aqua-MODIS in this region, which could lead to different DRE even if the same method was used.

5. Summary and Discussion

Recent advances in satellite-based remote sensing, in particular the launch of the space-borne lidar CALIOP, have provided an unprecedented opportunity for studying the radiative effects of above-cloud aerosol (ACA). However, the methodologies used in recent studies for computing the ACA DRE appear to be either oversimplified (e.g., Chand et al., 2009; Oikawa et al., 2013) or too cumbersome (e.g., Meyer et al., 2013). This paper describes a novel method recently developed for computing the shortwave

Zhibo Zhang 3/7/14 9:03 AM

Deleted: Recent studies found about a factor of two difference between CALIOP nighttime and daytime AOD retrievals (Chand et al., 2008; Meyer et al., 2013). If this difference is considered as CALIOP AOD retrieval uncertainty, it could lead to 30%~50% uncertainty in ACA DRE computation (see Fig. 12 of Meyer et al., 2013).

Zhibo Zhang 3/7/14 9:03 AM

Deleted: However, the methodologies used in recent studies for computing the ACA DRE appear to be either oversimplified (e.g., Chand et al., 2009; Oikawa et al., 2013) or too cumbersome (e.g., Meyer et al., 2013). This paper describes a novel method recently developed for computing the shortwave DRE of above-cloud aerosols over ocean. Our method has several unique features compared to methods used in previous studies: 1) It takes sub-grid scale cloud and aerosol variation into account in DRE computations, similar to(Meyer et al., 2013); 2) it also treats the overlapping of aerosol and cloud rigorously by utilizing the joint histogram of COD and CTP in the MODIS level-3 cloud product; 3) it differs from (Meyer et al., 2013) in its reliance on grid-level cloud statistics (i.e., COD-CTP joint histogram), instead of pixel-level products, and utilizes pre-computed look-up tables for ACA DRE computations, making it thus much more efficient than pixel-level computations. As shown in Figure 3, Figure 4 and Table 2, DRE computed using our method agrees well with the pixel-level computations in (Meyer et al., 2013).

DRE of above-cloud aerosols over ocean. Our method has several unique features compared to previous methods: 1) It takes sub-grid scale cloud and aerosol variation into account in DRE computations, similar to (Meyer et al., 2013); 2) it treats the overlap of aerosol and cloud rigorously by utilizing the joint histogram of COD and CTP in the MODIS level-3 cloud product; 3) it relies on grid-level cloud statistics (i.e., COD-CTP joint histogram), instead of pixel-level products, and utilizes pre-computed look-up tables for ACA DRE computations, making it thus much more efficient than pixel-level computations. As shown in Figure 3, Figure 4 and Table 2, DRE computed using our method agrees well with the pixel-level computations of (Meyer et al., 2013)..

In addition to the Southeast Atlantic region, we have recently begun investigating the DRE of above-cloud light-absorbing aerosols for global ocean. Some preliminary results are shown in Figure 5. We first derived the daily grid-level statistics of above-cloud AOD and below-cloud COD, as well as the corresponding ACA DRE, using the method described above and then aggregated the daily means to annual mean. The temporal aggregation is weighted by the number of ACA pixels in each day during 2007-2010. For example, the annual mean ACA DRE in Figure 5c is aggregated from daily mean based on the following equation:

$$\overline{\langle DRE \rangle_{ACA}} = \frac{\sum_i N_i \cdot \langle DRE_i \rangle_{ACA}}{\sum_i N_i}, \; i\text{=day 1, 2, 3…} \qquad (3)$$

where $\langle DRE_i \rangle_{ACA}$ is the spatially averaged instantaneous ACA DRE in each day averaged over ACA pixels, N_i is the number of ACA pixels in the grid box in each day, and $\overline{\langle DRE \rangle_{ACA}}$ is the annual mean instantaneous ACA DRE shown in Figure 5c. Figure 5a

Zhibo Zhang 3/7/14 9:03 AM
Deleted:

Unknown
Field Code Changed

Zhibo Zhang 3/7/14 9:03 AM
Deleted: mean

Zhibo Zhang 3/7/14 9:03 AM
Deleted: In

shows a global map of the annual mean 550 nm AOD of above cloud smoke and polluted dust derived based on 4 years (2007-2010) of CALIOP aerosol and cloud layer products. Similar to (Devasthale and Thomas, 2011), we note several "hotspots" of ACA over the Southeast Atlantic, the East-Central Atlantic off the western coast of Saharan Africa, the Arabian sea, and the North Pacific basin off the coast of eastern Asia. It is interesting to note that the ACA AOD over the east-central Atlantic and Arabian Sea is noticeably larger than that over the southeast Atlantic and North Pacific basin. Figure 5b shows the annual mean below-aerosol COD derived from the MODIS daily level-3 cloud product after the correction of above-cloud AOD contamination using the method described in section 3. A notable feature in the figure is that the below-aerosol COD over the North Pacific basin is significantly larger than that over other ACA regions. Figure 5c shows the annual mean shortwave DRE at TOA aggregated from daily values due to ACA smoke and polluted dust over the global ocean. It is intriguing to see that the DRE of ACA over the North Pacific basin is significantly larger than that over the southeast Atlantic, which is in turn larger than the DRE over the east-central Atlantic and the Arabian Sea. In fact, some negative DREs are observed in the latter two regions. This probably due to the COD of below-aerosol clouds being too thin (Figure 5b) over these regions to have significant radiative effect, so that the radiative effect of ACA is close to that of clear skies (i.e., negative). This is interesting because the above-cloud AOD over these regions is actually larger, while the below–aerosol COD over these regions is smaller, compared to their counterparts over the southeast Atlantic and North Pacific basin. Therefore, the preliminary results seem to suggest that the variability of DRE of ACA is modulated by COD, rather than AOD, although it should be noted that we have focused only on the light-absorbing aerosols, i.e., smoke and polluted dust, and assumed

Zhibo Zhang 3/7/14 9:03 AM
Deleted: is shown

Zhibo Zhang 3/7/14 9:03 AM
Deleted: Similar to (Devasthale and Thomas, 2011)

Zhibo Zhang 3/7/14 9:03 AM
Deleted: in comparison with the

Zhibo Zhang 3/7/14 9:03 AM
Deleted: smoke and polluted dust, and assumed the same broadband scattering properties for them as in (Meyer et al., 2013). Future

the same narrowband scattering properties for them as in (Meyer et al., 2013). Further research is needed to study the impact of aerosol type and scattering properties on the temporal-spatial variation of DRE on global scale. Nevertheless, the preliminary results shown Figure 5 clearly demonstrate the usefulness of our new method for global studies.

It should be noted that this study, and previous ones using CALIOP observations (e.g., Chand et al., 2008; Meyer et al., 2013; Oikawa et al., 2013), are limited by the capabilities of CALIOP. Arguably, some aerosols exist above every cloud. However, not all ACA can be detected by CALIOP due to its inherent limitations. Some ACAs are simply too optically thin to be detected, though their radiative effects are also expected to be small. Other situations may also be possible. For example, a confined aerosol layer has larger volume backscatter than a vertically stretched layer, even if the total aerosol amounts are the same, and therefore is more easily detected by CALIOP. Passive sensors, on the other hand, are less affected by the vertical distribution of ACA because they observe column-integrated scattering by aerosols. Recently, several novel techniques have been developed to detect and retrieve ACA properties using passive sensors. (Waquet et al., 2009) developed a method based on multi-angular polarization measurements from POLDER (Polarization and Directionality of the Earth Reflectances) to retrieve the AOD of above-cloud smoke. This method has recently been extended to include both smoke and dust aerosols (Waquet et al., 2013a). Most recently, (Jethva et al., 2013) demonstrated the ability of a color ratio method to retrieve the above-cloud AOD based on MODIS multiple spectral cloud reflectance measurements. A review of the emerging satellite-based observations of above-cloud aerosols can be found in (Yu and Zhang, 2013). The capabilities and limitations of the passive techniques need to be

Zhibo Zhang 3/7/14 9:03 AM
Deleted: study

Zhibo Zhang 3/7/14 9:03 AM
Deleted: (e.g., Chand et al., 2008; Meyer et al., 2013; Oikawa et al., 2013)

Zhibo Zhang 3/7/14 9:03 AM
Deleted: There are

Zhibo Zhang 3/7/14 9:03 AM
Deleted: other possibilities

Zhibo Zhang 3/7/14 9:03 AM
Deleted: (Waquet et al., 2009)

Zhibo Zhang 3/7/14 9:03 AM
Deleted: (Waquet et al., 2013). Most recently, (Jethva et al., 2013)

Zhibo Zhang 3/7/14 9:03 AM
Deleted: (Yu and Zhang, 2013).

systematically studied through inter-comparisons and comparison with CALIOP observations, but they may provide a complementary perspective on ACA. Recall that passive imagers have much larger spatial coverage than CALIOP, which makes brute force calculations of the DRE at the pixel level computationally expensive. In this regard, our method satisfies the need for efficiency of ACA DRE computations based on passive imager retrievals.

As a final remark, we would like to point out that the ACA DRE discussed in this study is still a few steps away from the all-sky aerosol radiative effect ($\langle DRE \rangle_{all-sky}$). For a given grid box, the $\langle DRE \rangle_{all-sky}$ can be decomposed into the sum of clear-sky and cloudy-sky DRE:

$$\langle DRE \rangle_{all-sky} = (1 - f_c) \cdot \langle DRE \rangle_{clear} + f_c \cdot f_{ACA} \cdot \langle DRE \rangle_{ACA}, \quad (4)$$

where f_c is the cloud fraction, $\langle DRE \rangle_{clear}$ is the DRE averaged over the clear-sky portion of the grid box, f_{ACA} is the fraction of cloudy pixels with ACA detected by CALIOP or other sensors, and $\langle DRE \rangle_{ACA}$ is the DRE averaged over all ACA containing pixels. It is important to note an implicit assumption made in Eq. (4), that is, when a distinct ACA layer is not detected, the DRE of ACA is zero. Different sensors (or different retrieval algorithms for the same sensor) may have different sensitivities to ACA and therefore provide different estimates of f_{ACA} and $\langle DRE \rangle_{ACA}$. For example, one sensor may only be able to retrieve ACA for optically thick clouds. This sensor would retrieve a larger $\langle DRE \rangle_{ACA}$, but a smaller f_{ACA}, in comparison with another sensor capable of retrieving ACA for all clouds. Therefore, when comparing the ACA or all-sky

Zhibo Zhang 3/7/14 9:03 AM
Deleted: comparison

Zhibo Zhang 3/7/14 9:03 AM
Deleted: Note

Unknown
Field Code Changed

Zhibo Zhang 3/7/14 9:03 AM
Deleted: that is able to retrieve

DRE estimated based on different instruments or algorithms, it is important to compare both the f_{ACA} and $\langle DRE \rangle_{ACA}$ terms in Eq. (4).

Table 1 Quality control metrics used for screening the CALIOP aerosol layer product.

	Criterion
CAD_score	< −30
Horizontal_averaging	< 20km
Extinction_QC_532	0 or 1
Feature_Optical_Depth_Uncertainty_532	< −99.5

Table 2 Regional and seasonal mean values of instantaneous DRE and RFE based on the pixel-level computation and the new method.

	DRE [W m^{-2}] Bias adjusted (unadjusted)	RFE [W m^{-2} AOD^{-1}] Bias adjusted (unadjusted)
Pixel computation	6.6 (5.92)	56.0 (50.3)
New Method	6.4 (5.77)	53.8 (50.2)

Zhibo Zhang 3/7/14 9:03 AM
Deleted: 63

Zhibo Zhang 3/7/14 9:03 AM
Deleted: 55.97

Zhibo Zhang 3/7/14 9:03 AM
Deleted: 34

Zhibo Zhang 3/7/14 9:03 AM
Deleted: 39

Zhibo Zhang 3/7/14 9:03 AM
Deleted: 77

Zhibo Zhang 3/7/14 9:03 AM
Deleted: 22

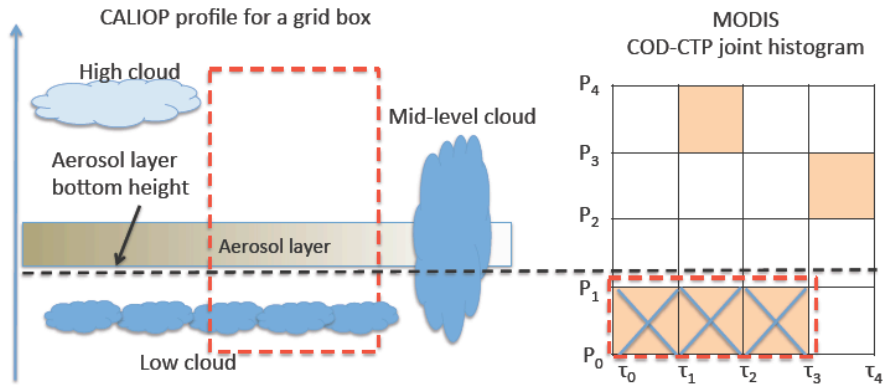

Figure 1 A schematic example to illustrate how CALIOP aerosol layer height information is used in our method to determine the population of liquid-phase clouds below the aerosol layer in the MODIS COD-CTP joint histogram.

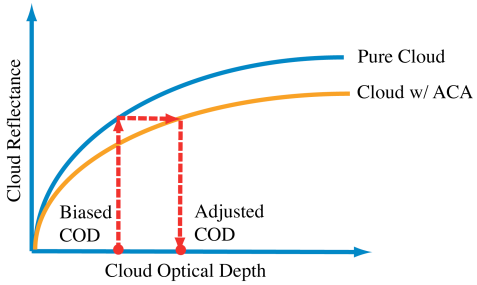

Figure 2 A schematic illustration of our fast scheme to correct the COD retrieval bias in the MODIS cloud product due to overlying aerosol contamination.

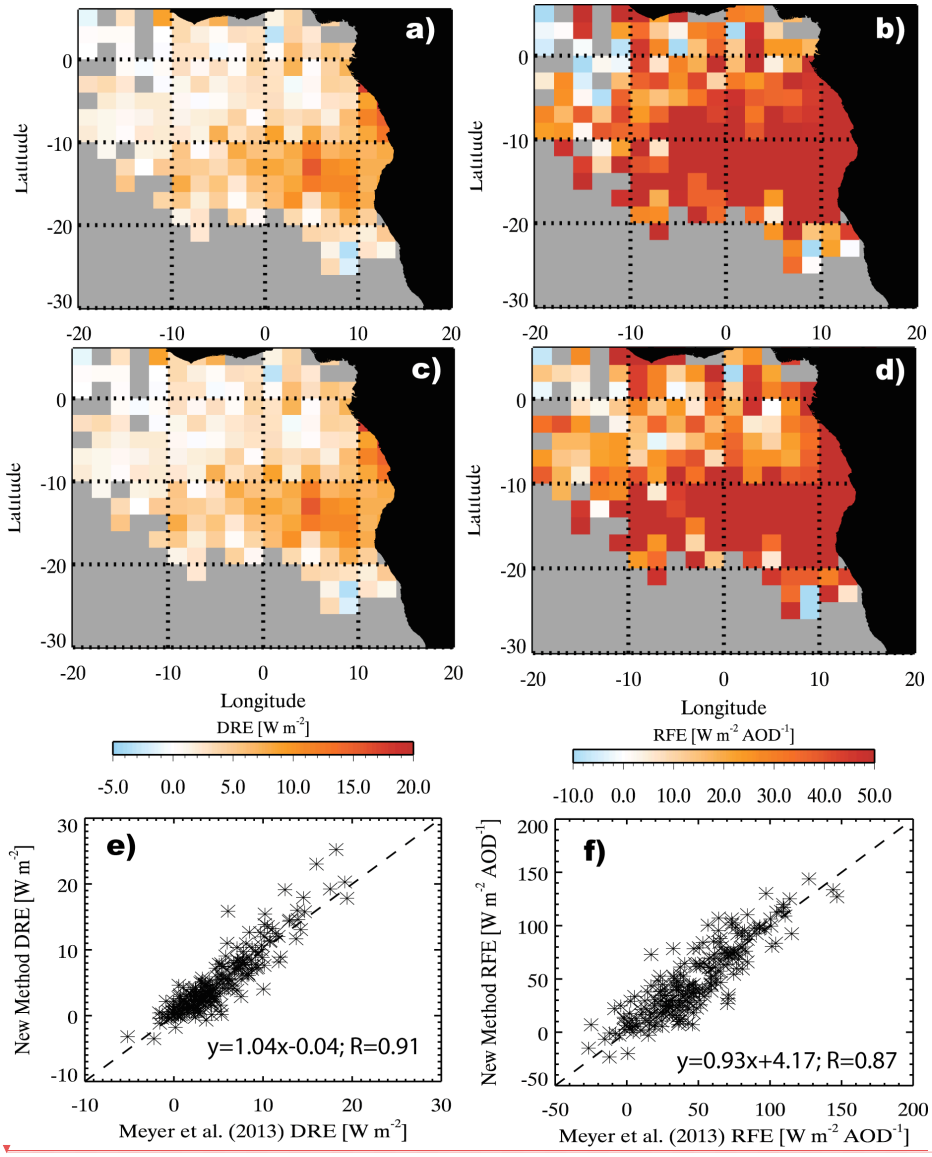

Figure 3 a) Seasonal mean (August/September 2007-2011) instantaneous TOA DRE of above-cloud smoke and polluted dust based on the pixel-level computations from (Meyer et al., 2013); b) seasonal mean instantaneous TOA aerosol RFE (i.e., DRE per AOD) from(Meyer et al., 2013); c) same as a), but based on the new method; d) same as b), but based on the new method.

Zhibo Zhang 3/7/14 9:03 AM

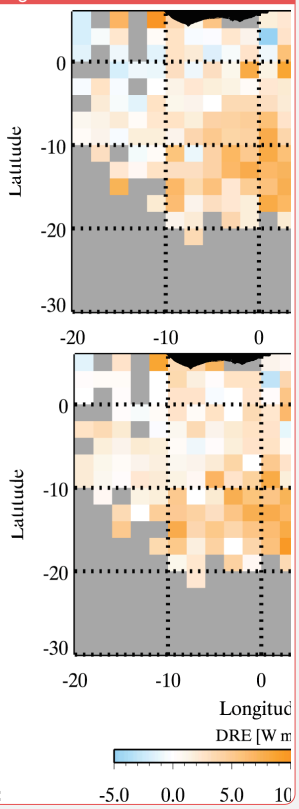

Deleted:

Zhibo Zhang 3/7/14 9:03 AM

Deleted: a) Seasonal mean (August/September 2007-2011) instantaneous TOA DRE of above-cloud smoke and polluted dust based on the pixel-level computations from (Meyer et al., 2013); b) seasonal mean instantaneous TOA aerosol RFE (i.e., DRE per AOD) from(Meyer et al., 2013); c) same as a), but based on the new method; d) same as b), but based on the new method. ... [6]

1
2
3
4
5
6

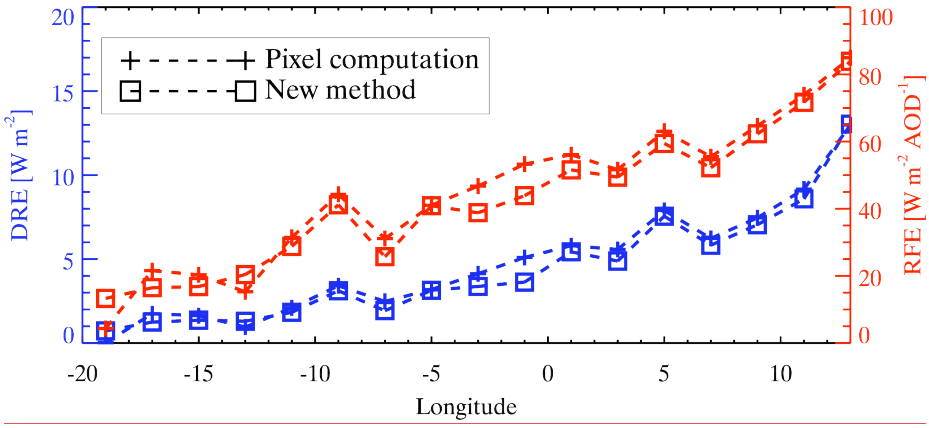

Figure 4 Meridional mean DRE and RFE for the region based on the results in Figure 3. Lines with cross symbol correspond to pixel computations from (Meyer et al., 2013). Lines with square symbol correspond to results based on the new method.

Zhibo Zhang 3/7/14 9:03 AM
Deleted: (Meyer et al., 2013)

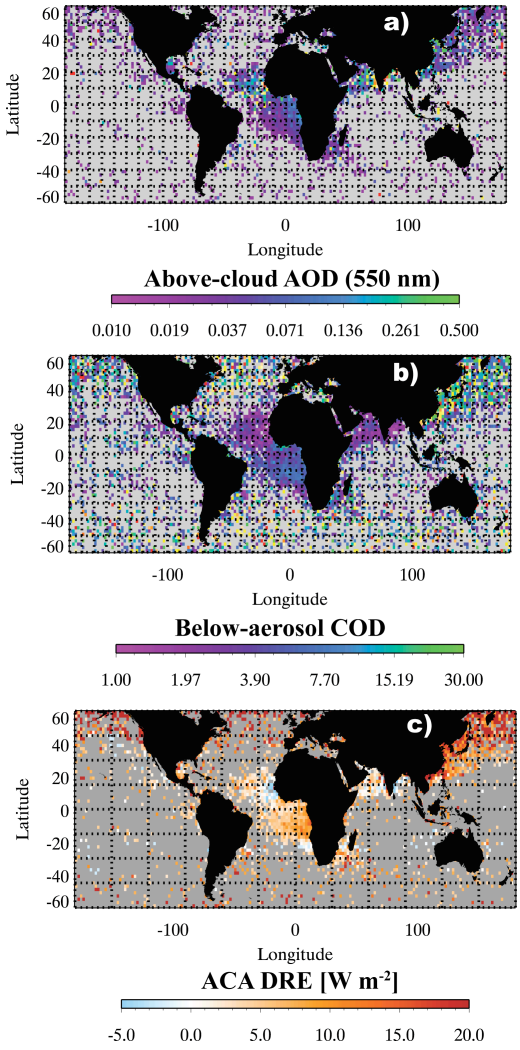

Figure 5 a) Annual mean AOD (at 550 nm) of above-cloud light-absorbing aerosols (i.e., smoke and polluted dust) derived from 4 years (2007~2010) of the CALIOP 5km aerosol and cloud layer products. b) Annual mean below-aerosol COD derived from the MODIS daily level-3 COD-CTP joint histogram. c) Annual mean instantaneous TOA DRE of above-cloud light-absorbing aerosols derived using the new method.

Reference:

Abel, S. J., Highwood, E. J., Haywood, J. M. and Stringer, M. A.: The direct radiative effect of biomass burning aerosols over southern Africa, Atmospheric Chemistry and Physics, 5(7), 1999–2018, doi:10.5194/acp-5-1999-2005, 2005.

Ackerman, S., Strabala, K., Menzel, W., Frey, R., Moeller, C. and Gumley, L.: Discriminating clear sky from clouds with MODIS, Journal of Geophysical Research, 103(D24), 32,141–32,157, 1998.

Bergman, J. W. and Salby, M. L.: Diurnal Variations of Cloud Cover and Their Relationship to Climatological Conditions, Journal of Climate, 9(11), 2802–2820, doi:10.1175/1520-0442(1996)009<2802:DVOCCA>2.0.CO;2, 1996.

Chand, D., Anderson, T. L., Wood, R., Charlson, R. J., Hu, Y., Liu, Z. and Vaughan, M.: Quantifying above-cloud aerosol using spaceborne lidar for improved understanding of cloudy-sky direct climate forcing, J Geophys Res, 113(D13), doi:10.1029/2007JD009433, 2008.

Chand, D., Wood, R., Anderson, T. L., Satheesh, S. K. and Charlson, R. J.: Satellite-derived direct radiative effect of aerosols dependent on cloud cover, Nature Geoscience, 2(3), 181–184, doi:10.1038/ngeo437, 2009.

Clough, S. A., Shephard, M. W., Mlawer, E. J., Delamere, J. S., Iacono, M. J., Cady-Pereira, K., Boukabara, S. and Brown, P. D.: Atmospheric radiative transfer modeling: a summary of the AER codes, Journal of Quantitative Spectroscopy and Radiative Transfer VL -, 91(2), 233–244, 2005.

Coddington, O. M., Pilewskie, P., Redemann, J., Platnick, S., Russell, P. B., Schmidt, K. S., Gore, W. J., Livingston, J., Wind, G. and Vukicevic, T.: Examining the impact of overlying aerosols on the retrieval of cloud optical properties from passive remote sensing, J Geophys Res, 115(D10), doi:10.1029/2009JD012829, 2010.

Costantino, L. and Bréon, F. M.: Aerosol indirect effect on warm clouds over South-East Atlantic, from co-located MODIS and CALIPSO observations, Atmospheric Chemistry and Physics, 13(1), 69–88, doi:10.5194/acp-13-69-2013, 2013a.

Costantino, L. and Bréon, F. M.: Satellite-based estimate of aerosol direct radiative effect over the South-East Atlantic, Atmospheric Chemistry and Physics Discussions, 13(9), 23295–23324, doi:10.5194/acpd-13-23295-2013, 2013b.

de Graaf, M., Tilstra, L. G., Wang, P. and Stammes, P.: Retrieval of the aerosol direct radiative effect over clouds from spaceborne spectrometry, J Geophys Res, 117(D7), doi:10.1029/2011JD017160, 2012.

Devasthale, A. and Thomas, M. A.: A global survey of aerosol-liquid water cloud overlap

based on four years of CALIPSO-CALIOP data, Atmospheric Chemistry and Physics, 11(3), 1143–1154, doi:10.5194/acp-11-1143-2011, 2011.

Eck, T. F., Holben, B. N., Ward, D. E., Mukelabai, M. M., Dubovik, O., Smirnov, A., Schafer, J. S., Hsu, N. C., Piketh, S. J., Queface, A., Roux, J. L., Swap, R. J. and Slutsker, I.: Variability of biomass burning aerosol optical characteristics in southern Africa during the SAFARI 2000 dry season campaign and a comparison of single scattering albedo estimates from radiometric measurements, J. Geophys. Res., 108(D13), 8477, doi:10.1029/2002JD002321, 2003.

Hartmann, D., Holton, J. and Fu, Q.: The heat balance of the tropical tropopause, cirrus, and stratospheric dehydration, Geophys Res Lett, 28(10), 1969–1972, 2001.

Haywood, J. M., Osborne, S. R. and Abel, S. J.: The effect of overlying absorbing aerosol layers on remote sensing retrievals of cloud effective radius and cloud optical depth, Quarterly Journal of the Royal Meteorological Society, 130(598), 779–800, doi:10.1256/qj.03.100, 2004.

Hu, Y., Vaughan, M., Liu, Z., Lin, B., Yang, P., Flittner, D., Hunt, B., Kuehn, R., Huang, J., Wu, D., Rodier, S., Powell, K., Trepte, C. and Winker, D.: The depolarization - attenuated backscatter relation: CALIPSO lidar measurements vs. theory, Opt. Express, 15(9), 5327, doi:10.1364/OE.15.005327, 2007a.

Hu, Y., Vaughan, M., Liu, Z., Powell, K. and Rodier, S.: Retrieving Optical Depths and Lidar Ratios for Transparent Layers Above Opaque Water Clouds From CALIPSO Lidar Measurements, Geoscience and Remote Sensing Letters, IEEE DOI - 10.1109/LGRS.2007.901085, 4(4), 523–526, 2007b.

Hubanks, P. A., King, M. D., Platnick, S. and Pincus, R.: MODIS atmosphere L3 gridded product algorithm theoretical basis document, Algorithm Theor. Basis Doc. ATBD-MOD, 30, 2008.

Iacono, M. J., Delamere, J. S., Mlawer, E. J., Shephard, M. W., Clough, S. A. and Collins, W. D.: Radiative forcing by long-lived greenhouse gases: Calculations with the AER radiative transfer models, J. Geophys. Res., 113(D13), D13103, doi:10.1029/2008JD009944, 2008.

Ichoku, C., Remer, L. A., Kaufman, Y. J., Levy, R., Chu, D. A., Tanré, D. and Holben, B. N.: MODIS observation of aerosols and estimation of aerosol radiative forcing over southern Africa during SAFARI 2000, J. Geophys. Res., 108(D13), 8499, doi:10.1029/2002JD002366, 2003.

Jethva, H., Torres, O., Remer, L. A. and Bhartia, P. K.: A color ratio method for simultaneous retrieval of aerosol and cloud optical thickness of above-cloud absorbing aerosols from passive sensors: Application to MODIS measurements, IEEE TRANSACTIONS ON GEOSCIENCE AND REMOTE SENSING, 51(7), 3862–3870, 2013.

Zhibo Zhang 3/7/14 9:03 AM
Deleted: 2007

Jethva, H., Torres, O., Waquet, F., Chand, D. and Hu, Y.: How do A-train sensors intercompare in the retrieval of above-cloud aerosol optical depth? A case study-based assessment, Geophysical Research Letters, n/a–n/a, doi:10.1002/2013GL058405, 2014.

Keil, A. and Haywood, J. M.: Solar radiative forcing by biomass burning aerosol particles during SAFARI 2000: A case study based on measured aerosol and cloud properties, J Geophys Res, 108(D13), 8467, doi:10.1029/2002JD002315, 2003.

King, M. D., Platnick, S., Menzel, W. P., Ackerman, S. A. and Hubanks, P. A.: Spatial and Temporal Distribution of Clouds Observed by MODIS Onboard the Terra and Aqua Satellites, IEEE TRANSACTIONS ON GEOSCIENCE AND REMOTE SENSING, 51(7), 3826–3852, doi:10.1109/TGRS.2012.2227333, 2013.

Kistler, R., Collins, W., Saha, S., White, G., Woollen, J., Kalnay, E., Chelliah, M., Ebisuzaki, W., Kanamitsu, M., Kousky, V., van den Dool, H., Jenne, R. and Fiorino, M.: The NCEP–NCAR 50–Year Reanalysis: Monthly Means CD–ROM and Documentation, Bulletin of the American Meteorological Society, 82(2), 247–267, doi:10.1175/1520-0477(2001)082<0247:TNNYRM>2.3.CO;2, 2001.

Levy, R. C., Remer, L. A., Tanre, D., Mattoo, S. and Kaufman, Y. J.: Algorithm for remote sensing of tropospheric aerosol over dark targets from MODIS: Collections 005 and 051: Revision 2, MODIS Algorithm Theoretical Basis Document for the MOD04_L2 Product, 2009.

Liu, Z., Vaughan, M., Winker, D., Kittaka, C., Getzewich, B., Kuehn, R., Omar, A., Powell, K., Trepte, C. and Hostetler, C.: The CALIPSOLidar Cloud and Aerosol Discrimination: Version 2 Algorithm and Initial Assessment of Performance, Journal of Atmospheric and Oceanic Technology, 26(7), 1198–1213, doi:10.1175/2009JTECHA1229.1, 2009.

Liu, Z., Winker, D. M., Omar, A. H., Vaughan, M., Kar, J., Trepte, C. R. and Hu, Y.: Evaluation of CALIOP 532-nm AOD over Clouds, AGU Fall Meeting 2013, 2013.

Menzel, P., Frey, R., Baum, B. and Zhang, H.: Cloud Top Properties and Cloud Phase Algorithm Theoretical Basis Document. 2006.

Menzel, W., Smith, W. and Stewart, T.: Improved Cloud Motion Wind Vector and Altitude Assignment Using VAS, Journal of Applied Meteorology, 22(3), 377–384, 1983.

Meyer, K., Platnick, S., Oreopoulos, L. and Lee, D.: Estimating the direct radiative effect of absorbing aerosols overlying marine boundary layer clouds in the southeast Atlantic using MODIS and CALIOP, Journal of Geophysical Research-Atmospheres, n/a–n/a, doi:10.1002/jgrd.50449, 2013.

Min, M. and Zhang, Z.: **On the influence of cloud fraction diurnal cycle and sub-grid cloud optical thickness variability on all-sky direct aerosol radiative forcing**

Zhibo Zhang 3/7/14 9:03 AM

Deleted: Menzel, W. P., Kaufman, Y. J., Tanre, D., Gao, B.-C., Platnick, S., Ackerman, S. A., Remer, L. A., Pincus, R. and Hubanks, P. A.: Cloud and aerosol properties, precipitable water, and profiles of temperature and water vapor from MODIS, Geoscience and Remote Sensing, IEEE Transactions on, 41(2), 442–458, doi:10.1109/TGRS.2002.808226, 2003. ... [7]

, Journal of Quantitative Spectroscopy and Radiative Transfer, ((submitted)), n.d.

Myhre, G., Berntsen, T. K., Haywood, J. M., Sundet, J. K., Holben, B. N., Johnsrud, M. and Stordal, F.: Modeling the solar radiative impact of aerosols from biomass burning during the Southern African Regional Science Initiative (SAFARI-2000) experiment, J. Geophys. Res., 108(D13), 8501, doi:10.1029/2002JD002313, 2003.

Nakajima, T. and King, M.: Determination of the optical thickness and effective particle radius of clouds …, J Atmosph Sci, 1990.

Oikawa, E., Nakajima, T., Inoue, T. and Winker, D.: A study of the shortwave direct aerosol forcing using ESSP/CALIPSO observation and GCM simulation, J Geophys Res, 118, 3687–3708, doi:10.1002/jgrd.50227, 2013.

Omar, A. H., Winker, D. M., Vaughan, M. A., Hu, Y., Trepte, C. R., Ferrare, R. A., Lee, K.-P., Hostetler, C. A., Kittaka, C. and Rogers, R. R.: The CALIPSO automated aerosol classification and lidar ratio selection algorithm, Journal of Atmospheric and Oceanic Technology, 26(10), 1994–2014, 2009.

Oreopoulos, L., Cahalan, R. F. and Platnick, S.: The Plane-Parallel Albedo Bias of Liquid Clouds from MODIS Observations, Journal of Climate, 20(20), 5114–5125, doi:10.1175/JCLI4305.1, 2007.

Platnick, S., King, M., Ackerman, S., Menzel, W., Baum, B., Riedi, J. and Frey, R.: The MODIS cloud products: algorithms and examples from Terra, Geoscience and Remote Sensing, IEEE Transactions on, 41(2), 459–473, 2003.

Rossow, W. B. and Schiffer, R. A.: Advances in Understanding Clouds from ISCCP, Bulletin of the American Meteorological Society, 80(11), 2261–2287, doi:10.1175/1520-0477(1999)080<2261:AIUCFI>2.0.CO;2, 1999.

Rozendaal, M. A., Leovy, C. B. and Klein, S. A.: An Observational Study of Diurnal Variations of Marine Stratiform Cloud, Journal of Climate, 8, 1795–1809, 1995.

Schulz, J., Albert, P., Behr, H. D., Caprion, D., Deneke, H., Dewitte, S., Dürr, B., Fuchs, P., Gratzki, A., Hechler, P., Hollmann, R., Johnston, S., Karlsson, K. G., Manninen, T., Müller, R., Reuter, M., Riihelä, A., Roebeling, R., Selbach, N., Tetzlaff, A., Thomas, W., Werscheck, M., Wolters, E. and Zelenka, A.: Operational climate monitoring from space: the EUMETSAT Satellite Application Facility on Climate Monitoring (CM-SAF), Atmospheric Chemistry and Physics, 9(5), 1687–1709, doi:10.5194/acp-9-1687-2009, 2009.

Schulz, M., Textor, C., Kinne, S., Balkanski, Y., Bauer, S., Berntsen, T., Berglen, T., Boucher, O., Dentener, F., Guibert, S., Isaksen, I. S. A., Iversen, T., Koch, D., Kirkevåg, A., Liu, X., Montanaro, V., Myhre, G., Penner, J. E., Pitari, G., Reddy, S., Seland, Ø., Stier, P. and Takemura, T.: Radiative forcing by aerosols as derived from the AeroCom present-day and pre-industrial simulations, Atmos. Chem. Phys, 6, 5225–5246, 2006.

Stier, P., Schutgens, N. A. J., Bellouin, N., Bian, H., Boucher, O., Chin, M., Ghan, S., Huneeus, N., Kinne, S., Lin, G., Ma, X., Myhre, G., Penner, J. E., Randles, C. A., Samset, B., Schulz, M., Takemura, T., Yu, F., Yu, H. and Zhou, C.: Host model uncertainties in aerosol radiative forcing estimates: results from the AeroCom Prescribed intercomparison study, Atmospheric Chemistry and Physics, 13(6), 3245–3270, doi:10.5194/acp-13-3245-2013, 2013.

Torres, O., Jethva, H. and Bhartia, P. K.: Retrieval of Aerosol Optical Depth above Clouds from OMI Observations: Sensitivity Analysis and Case Studies, http://dx.doi.org/10.1175/JAS-D-11-0130.1, 69(3), 1037–1053, doi:10.1175/JAS-D-11-0130.1, 2012.

Twomey, S.: Atmospheric aerosols, Elsevier Scientific Publishing Co.,New York, NY. 1977.

Vaughan, M. A., Powell, K. A., Winker, D. M., Hostetler, C. A., Kuehn, R. E., Hunt, W. H., Getzewich, B. J., Young, S. A., Liu, Z. and McGill, M. J.: Fully Automated Detection of Cloud and Aerosol Layers in the CALIPSO Lidar Measurements, J. Atmos. Oceanic Technol., 26(10), 2034–2050, doi:doi: 10.1175/2009JTECHA1228.1, 2009.

Waquet, F., Cornet, C., Deuzé, J. L., Dubovik, O., Ducos, F., Goloub, P., Herman, M., Lapyonok, T., Labonnote, L. C., Riedi, J., Tanre, D., Thieuleux, F. and Vanbauce, C.: Retrieval of aerosol microphysical and optical properties above liquid clouds from POLDER/PARASOL polarization measurements, Atmos. Meas. Tech., 6(4), 991–1016, doi:10.5194/amt-6-991-2013, 2013a.

Waquet, F., Peers, F., Ducos, F., Goloub, P., Platnick, S., Riedi, J., Tanré, D. and Thieuleux, F.: Global analysis of aerosol properties above clouds, Geophysical Research Letters, n/a–n/a, doi:10.1002/2013GL057482, 2013b.

Waquet, F., Riedi, J., Labonnote, L. C., Goloub, P., Cairns, B., Deuzé, J. L. and Tanre, D.: Aerosol Remote Sensing over Clouds Using A-Train Observations, J Atmosph Sci, 66(8), 2468–2480, doi:10.1175/2009JAS3026.1, 2009.

Wilcox, E. M.: Stratocumulus cloud thickening beneath layers of absorbing smoke aerosol, Atmospheric Chemistry and Physics, 10(23), 11769–11777, doi:10.5194/acp-10-11769-2010, 2010.

Wilcox, E. M.: Direct and semi-direct radiative forcing of smoke aerosols over clouds, Atmospheric Chemistry and Physics, 12(1), 139–149, doi:10.5194/acp-12-139-2012, 2012.

Winker, D. M., Tackett, J. L., Getzewich, B. J., Liu, Z., Vaughan, M. A. and Rogers, R. R.: The global 3-D distribution of tropospheric aerosols as characterized by CALIOP, Atmospheric Chemistry and Physics, 13(6), 3345–3361, doi:10.5194/acp-13-3345-2013, 2013.

Winker, D. M., Vaughan, M. A., Omar, A., Hu, Y., Powell, K. A., Liu, Z., Hunt, W. H.

Zhibo Zhang 3/7/14 9:03 AM
Deleted: osti.gov,

Zhibo Zhang 3/7/14 9:03 AM
Deleted: 2013

and Young, S. A.: Overview of the CALIPSO mission and CALIOP data processing algorithms, Journal of Atmospheric and Oceanic Technology, 26(11), 2310–2323, 2009.

Wiscombe, W. J.: Improved Mie scattering algorithms, Applied Optics, 19(9), 1505–1509, 1980.

Wood, R., Bretherton, C. S. and Hartmann, D. L.: Diurnal cycle of liquid water path over the subtropical and tropical oceans, Geophysical Research Letters, 29(23), 2092–, doi:10.1029/2002GL015371, 2002.

Young, S. A. and Vaughan, M. A.: The Retrieval of Profiles of Particulate Extinction from Cloud-Aerosol Lidar Infrared Pathfinder Satellite Observations (CALIPSO) Data: Algorithm Description, J. Atmos. Oceanic Technol., 26(6), 1105–1119, doi:doi: 10.1175/2008JTECHA1221.1, 2008.

Yu, H. and Zhang, Z.: New Directions: Emerging satellite observations of above-cloud aerosols and direct radiative forcing, Atmospheric Environment, 72(0), 36–40, doi:10.1016/j.atmosenv.2013.02.017, 2013.

Yu, H., Kaufman, Y. J., Chin, M., Feingold, G., Remer, L. A., Anderson, T. L., Balkanski, Y., Bellouin, N., Boucher, O. and Christopher, S.: A review of measurement-based assessments of the aerosol direct radiative effect and forcing, Atmospheric Chemistry and Physics, 6(3), 613–666, 2006.

Zelinka, M. D., Klein, S. A. and Hartmann, D. L.: Computing and partitioning cloud feedbacks using cloud property histograms. Part I: Cloud radiative kernels, Journal of Climate, 25(11), 3715–3735, doi:10.1175/JCLI-D-11-00248.1, 2012.

Zhibo Zhang 3/7/14 9:03 AM
Deleted: J.